



ΠΑΝΕΠΙΣΤΗΜΙΟ ΙΩΑΝΝΙΝΩΝ
ΤΜΗΜΑ ΜΑΘΗΜΑΤΙΚΩΝ



Μιχαήλ Καραντώνης

Τύρβη και Διαλειπότητα

ΜΕΤΑΠΤΥΧΙΑΚΗ ΔΙΑΤΡΙΒΗ

Ιωάννινα, 2025



UNIVERSITY OF IOANNINA
Department of Mathematics



Mixail Karantonis

Turbulence and Intermittency

Master's Thesis

Ioannina, 2025

Στην οικογένειά μου.

Η παρούσα Μεταπτυχιακή Διατριβή εκπονήθηκε στο πλαίσιο των σπουδών για την απόκτηση του Μεταπτυχιακού Διπλώματος Ειδίκευσης στα Εφαρμοσμένα Μαθηματικά και Πληροφορική που απονέμει το Τμήμα Μαθηματικών του Πανεπιστημίου Ιωαννίνων.

Εγκρίθηκε την 27/6/2025 από την εξεταστική επιτροπή:

Όνοματεπώνυμο	Βαθμίδα
Μιχαήλ Ξένος	Καθηγητής
Θεόδωρος Χωρίκης	Καθηγητής
Γεώργιος Κανελλόπουλος	Επίκουρος Καθηγητής

ΥΠΕΥΘΥΝΗ ΔΗΛΩΣΗ

“Δηλώνω υπεύθυνα ότι η παρούσα διατριβή εκπονήθηκε κάτω από τους διεθνείς ηθικούς και ακαδημαϊκούς κανόνες δεοντολογίας και προστασίας της πνευματικής ιδιοκτησίας. Σύμφωνα με τους κανόνες αυτούς, δεν έχω προβεί σε ιδιοποίηση ξένου επιστημονικού έργου και έχω πλήρως αναφέρει τις πηγές που χρησιμοποίησα στην εργασία αυτή.”

Μιχαήλ Καραντώνης

ΕΥΧΑΡΙΣΤΙΕΣ

Η παρούσα διατριβή εκπονήθηκε στα πλαίσια του Μεταπτυχιακού Διπλώματος Ειδίκευσης "Εφαρμοσμένα Μαθηματικά και Πληροφορική" του τμήματος Μαθηματικών, Πανεπιστημίου Ιωαννίνων, με επιβλέποντα τον Καθηγητή κ. Μιχαήλ Ξένο και μέλη της τριμελούς Εξεταστικής Επιτροπής κ. Θεόδωρο Χωρίκη και κ. Γεώργιο Κανελλόπουλο.

Ευχαριστώ θερμά τον κ. Μιχαήλ Ξένο για τη πολύτιμη βοήθεια και τις συμβουλές που μου προσέφερε για την εκπόνηση αυτής της διατριβής. Τον ευχαριστώ για την καθοδήγηση και την στήριξη που μου προσέφερε κατά τη διάρκεια της διατριβής. Στη συνέχεια θέλω να ευχαριστήσω τον κ. Κατσούδα Σπυρίδων για το χρόνο και τη βοήθεια που κατέβαλε για την εκπόνηση αυτής της διατριβής.

Επίσης, ευχαριστώ θερμά τους, κ. Θεόδωρο Χωρίκη, Καθηγητή του τμήματος Μαθηματικών του Πανεπιστημίου Ιωαννίνων και κ. Γεώργιο Κανελλόπουλο, Επίκουρο Καθηγητή του Τμήματος Μαθηματικών του Πανεπιστημίου Πατρών, για την προθυμία τους να συμμετάσχουν στην Τριμελή Εξεταστική Επιτροπή και για τις πολύτιμες και εύστοχες παρατηρήσεις τους στην παρούσα εργασία.

Τέλος, θέλω να ευχαριστήσω τους γονείς μου, Ευστράτιο Καραντώνη και Ειρήνη Μαστροσάββα, για την αμέριστη αγάπη, κατανόηση και στήριξη τους καθ' όλη την ακαδημαϊκή καριέρα μου.

ΠΕΡΙΛΗΨΗ

Η παρούσα διπλωματική εργασία εστιάζει στη μελέτη της χρονοεξαρτώμενης τυρβώδους ροής και του φαινομένου της διαλειπτότητας της τύρβης. Δηλαδή, της χρονικής μετάβασης της ροής από στρωτή σε τυρβώδη και αντίστροφα, όπου αποτελεί ένα επαναλαμβανόμενο φαινόμενο στη φύση και σχετίζεται με μεγάλες απώλειες ενέργειας.

Η εξίσωση Burgers είναι ένα 1+1 διαστάσεων μοντέλο, το οποίο περιλαμβάνει τη βασική δομή των εξισώσεων Navier-Stokes (N-S). Επίσης, είναι ένα θεμελιώδες εργαλείο για τη μελέτη της μη γραμμικής δυναμικής σε συνδυασμό με την τυρβώδη ροή. Στην εργασία αυτή αναλύεται η συμπεριφορά της εξίσωσης Burgers, επικεντρώνοντας την προσοχή στον χώρο φάσεων, ο οποίος αποκαλύπτει τα χαρακτηριστικά των μεταβάσεων μεταξύ διαφορετικών περιοχών της ροής (μετάβαση από στρωτή σε τυρβώδη).

Επιπλέον, στην διατριβή αναλύονται οι διδιάστατες εξισώσεις Navier-Stokes οι οποίες λύνονται αριθμητικά με την εφαρμογή της μεθόδου των πεπερασμένων όγκων. Με τη χρήση προηγμένων μαθηματικών μεθόδων επίλυσης και διακριτοποίησης των εξισώσεων εξάγονται τα αποτελέσματα τα οποία περιλαμβάνουν την παρουσίαση του χώρου φάσεων ο οποίος βοηθά στην κατανόηση των δυναμικών λύσεων της εξίσωσης και από τις αριθμητικές λύσεις χρονοεξαρτώμενης ροής σε σωλήνα με χρήση εξελιγμένων μοντέλων τύρβης.

Η παρούσα εργασία συμβάλλει στην καλύτερη κατανόηση των αποτελεσμάτων τυρβώδους ροής σε χρονοεξαρτώμενες περιπτώσεις και προσφέρει μια συνεκτική μεθοδολογία για την αριθμητική επίλυση των σχετικών εξισώσεων.

ABSTRACT

This thesis focuses on the study of time-dependent turbulent flow and the phenomenon of turbulence intermittency. Intermittency is characterized by randomly alternations between deterministic and chaotic phases. Turbulence is a phenomenon that is pervasive in nature and is associated with large energy losses.

The Burgers equation is a simplification of the Navier-Stokes (N-S) equations, serving as a fundamental tool for the study of nonlinear dynamics coupled with turbulent flow. In this study, the behavior of the Burgers equation is analyzed, focusing on the phase space, which reveals the characteristics of the transitions between different regions of the flow (transition from laminar to turbulent).

In addition, the thesis analyzes the two-dimensional Navier-Stokes equations which are solved numerically by applying the finite volume method. By using advanced mathematical methods for solving and discretizing the equations, the results are extracted which consist of the phase space representation that helps in understanding the dynamic solutions of the equation and the numerical solutions of time-dependent flow in a channel using sophisticated and advanced turbulence models.

The present study contributes to a better understanding of turbulent flow in time-dependent scenarios and offers a coherent methodology for the numerical solution of the relevant equations.

CONTENTS

1	Introduction	3
1.1	Introduction-Historical review	3
1.2	Laminar Flow	3
1.3	Transition from Laminar to Turbulent Flow	4
1.4	The phenomenon of Turbulence	5
1.5	The phenomenon of Intermittency	7
2	Mathematical Background	11
2.1	Dynamical systems and Phase space	11
2.2	Energy Cascade and Kolmogorov Theory	14
2.2.1	Kolmogorov's scale	14
2.2.2	Kolmogorov's -5/3 Law	16
2.3	Turbulence Models	16
2.3.1	The k-ω Model	19
3	The Burgers' Equation	21
3.1	The inviscid Burgers' Equation	22
3.1.1	The method of characteristics	22
3.2	Analytical Solution of the homogeneous Burgers' Equation	24
3.2.1	Linearization of the Burgers' Equation	27
3.2.2	Non-homogeneous Case with Forcing Term $f(x, t) =$ $g(x)f(t)$	28

3.3	Solutions of the Burgers' Equation	29
3.3.1	Numerical solution of the non-homogeneous Burgers' equation	30
3.4	Intermittency in Burgers' Equation	31
3.5	Turbulent Burgers' Equation	32
4	Numerical solutions of the Navier-Stokes(N-S) Equations in turbulent internal flows	35
4.1	Couette and Hagen-Poiseuille flows	35
4.1.1	Couette flow	36
4.1.2	Hagen-Poiseuille flow	39
4.2	Turbulent Channel flow with k - ω model	42
4.3	The Finite Volume Method (FVM)	42
4.3.1	Results in Turbulent Channel	46
4.4	Solving the unsteady turbulent Navier-Stokes (URANS)	49
4.4.1	CFL Criterion	51
4.4.2	Numerical results	51
5	CONCLUSIONS	55
A	Appendix	57
A.1	URANS Discretization	57
A.2	k - ω Turbulence model Cartesian Form	60
A.3	Discretization of k - ω equations	61
A.3.1	Discretization of k equation	61
A.4	Discretization of ω equation	63
	References	67

CHAPTER 1

INTRODUCTION

1.1 Introduction-Historical review

Fluid dynamics has a rich and extensive history, with major developments appearing in the 17th century. Leonhard Euler laid the groundwork with his formulation of the Euler equations. These equations show the motion of inviscid fluids. In the beginning of the 19th century, Claude-Louis Navier and George Stokes extended Euler's equations including the term of viscosity μ , which led to the formulation of the Navier-Stokes (N-S) equations. During the 20th century, computational fluid dynamics (CFD) provided new approaches to simulate laminar and turbulent flows. In the mid-20th century, the concept of Intermittency started to appear as an extension of the Kolmogorov turbulence theory.

1.2 Laminar Flow

Laminar flow in channels occurs when a fluid flows in parallel layers without any macroscopic mixing. There are no cross-currents perpendicular to the direction of the flow, nor eddies or swirls of fluid flow. Laminar flow occurs primarily when we have low velocities and its viscosity forces dominate over the inertial forces. As a result, it has relatively small Reynolds number. Because of its nature, we can predict the behavior of a laminar flow, making it ideal for systems that require precise control over the flow. In the laminar flow we also have less energy loss compared to the turbulent flow, because laminar flow most of the times doesn't have eddies that cause additional energy losses to the fluid flow. The equations that describe the motion of viscous fluids are the Navier-Stokes equations. In vector form, the system of equations that describe the laminar flow of homogeneous, incompressible and viscous fluids

has the following formulation:

$$\frac{D\mathbf{q}}{Dt} = \mathbf{F} - \frac{1}{\rho}\nabla p + \nu\nabla^2\mathbf{q}, \quad (1.1)$$

where $\mathbf{q} = (u, v, w)$ is the velocity vector, \mathbf{F} is the body force vector, p is the pressure, ρ is the density, ν is the kinematic viscosity of the fluid and $\frac{D}{Dt}$ is the material derivative (known as Stokes operator), defined as:

$$\frac{D\mathbf{q}}{Dt} = \frac{\partial\mathbf{q}}{\partial t} + (\mathbf{q} \cdot \nabla) \cdot \mathbf{q} \quad (1.2)$$

The first term $\frac{\partial\mathbf{q}}{\partial t}$ is the local derivative and it is the time-dependent term of the flow. The term $(\mathbf{q} \cdot \nabla) \cdot \mathbf{q}$ represents the change of velocity due to the motion of the fluid itself and it is called convective derivative. We can write the Navier-Stokes equations in Cartesian coordinates as follows [2]:

$$\frac{\partial u}{\partial x} + \frac{\partial v}{\partial y} = 0, \quad \text{continuity equation} \quad (1.3)$$

$$u\frac{\partial u}{\partial x} + v\frac{\partial u}{\partial y} = F_x - \frac{1}{\rho}\frac{\partial p}{\partial x} + \nu\left(\frac{\partial^2 u}{\partial x^2} + \frac{\partial^2 u}{\partial y^2}\right), \quad \text{x-momentum} \quad (1.4)$$

$$u\frac{\partial v}{\partial x} + v\frac{\partial v}{\partial y} = F_y - \frac{1}{\rho}\frac{\partial p}{\partial y} + \nu\left(\frac{\partial^2 v}{\partial x^2} + \frac{\partial^2 v}{\partial y^2}\right), \quad \text{y-momentum} \quad (1.5)$$

The system of PDEs (1.3 - 1.5) describes the homogeneous, incompressible, viscous two-dimensional flow of a fluid. On the left-hand side of the system we have the inertial (convective) terms and on the right-hand side of the system appear the viscous diffusion terms, the body forces and the pressure gradient.

1.3 Transition from Laminar to Turbulent Flow

The concept of the Reynolds number (Re) is associated with Sir Osborne Reynolds (1842-1912). In 1883 he published a study in which he introduced the dimensionless quantity known as Reynolds number in order to investigate the transition of channel flow from laminar to turbulent. The term "Reynolds number" was coined by Arnold Summerfeld in 1908, in honor of Osborne Reynolds. A lot of studies have demonstrated that Reynolds number plays a significant role in fluid dynamics, as it accounts for the effects of viscosity and inertia. Reynolds number is a dimensionless quantity which is used to determine whether the fluid flow is laminar or turbulent [1]. It is the ratio

of the inertial forces to the viscous forces. Inertial forces oppose a change in the velocity of an object and play a key role in fluid motion. These forces are dominant in turbulent flow. Otherwise, if the viscous forces, which are defined as the resistance of the flow, are dominant the flow is laminar.

The dimensionless Reynolds number is given by the following formula:

$$Re = \frac{\text{inertial forces}}{\text{viscous forces}} = \frac{uL}{\nu},$$

where

- u : the characteristic velocity of the flow
- L : the characteristic length scale of the flow
- ν : the kinematic viscosity

The applicability of the Reynolds number varies depending on the specific characteristics of the fluid flow and whether the flow is internal or external. The critical Reynolds number indicates the threshold at which the flow transitions between different regimes. For example, while the critical Reynolds number for turbulent flow in a channel is approximately 2.300, for turbulent flow over a flat plate with free-stream velocity, it typically ranges from 4×10^5 to 4×10^6 [27].

At first, when the Reynolds number is relatively low (below 2.300 for channel flow), the flow is laminar which means that is characterized by smooth, parallel layers of fluid. As the Reynolds number increases small disturbances will grow, leading to the creation of eddies and turbulence. In between of the laminar flow and the turbulent flow there is another region called transitional. The transitional region occurs when the Reynolds number is between 2.300 and 4.000 in channel flow. In this region, the flow is unstable and small disturbances begin to grow. However, the flow has not fully transitioned into turbulence.

1.4 The phenomenon of Turbulence

Turbulent flow is a phenomenon that is pervasive in nature and in our daily life. Its mathematical description is particularly complex and unclear, reflecting the deep difficulties that arise when we try to describe three-dimensional

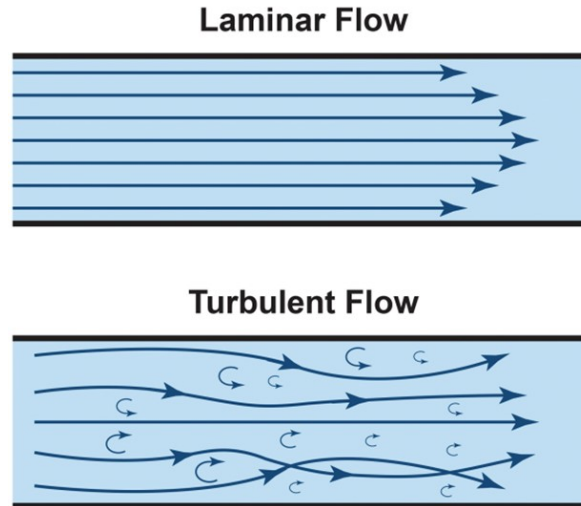


Figure 1.1: Representation of laminar and turbulent flow, in a channel.

chaotic flows. This fact has led many scientists to study it for centuries and have created many theories about it [6]. Several very famous scientists who studied the phenomenon are Kolmogorov, Boussinesq, Prandtl and Reynolds. Some of the most important contributions to the understanding of turbulent flow include Kolmogorov's theory of energy distribution at smaller scales, as well as the semi-empirical models that have been proposed for the analysis of diffusion and mixing in turbulent flows [18].

Despite the fact that the equations governing turbulence have been known since 1845, our ability to accurately predict its characteristics is limited. Turbulent flow is described as a state of flow where velocity and pressure exhibit random and chaotic fluctuations around a mean value, in contrast to the smooth and predictable behavior of laminar flow. High Reynolds number values coexist with this phenomenon. Eddies on various scales are created in turbulent flow and the process, named energy cascade, is the breaking down of large-scale energy to smaller scale. This dissipation of energy ultimately leads to its dissipation through the flow viscosity. The nature of turbulent flow leads to intense diffusion of momentum, heat and other properties, making it particularly important for applications such as aerodynamics, meteorology and chemical engineering.

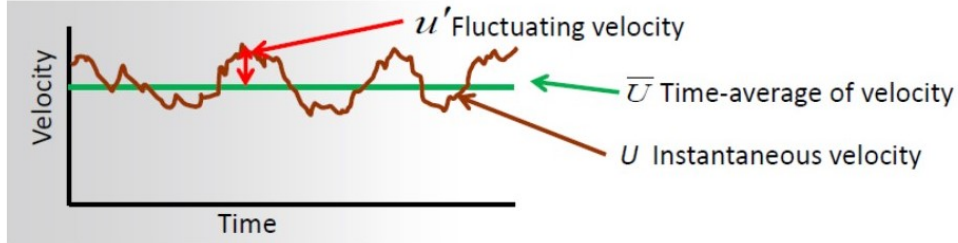


Figure 1.2: Velocity decomposition of U : \bar{U} is the time-average of velocity and U' is the fluctuations around the mean value ($U = \bar{U} + U'$)



Figure 1.3: The famous painting inspired by Vincent van Gogh called “Starry Night” (1889), presenting the chaotic eddies occurring in the night sky.

1.5 The phenomenon of Intermittency

In many applications, the governing equations involve certain parameters that may take different values from state to state [25]. Therefore, we refer to dynamic systems of the following form:

$$\dot{x} = \mathbf{f}(\mathbf{x}; \boldsymbol{\alpha}), \quad \mathbf{x} \in E^n, \quad \boldsymbol{\alpha} \in \mathbb{R}^k \quad (1.6)$$

where $\boldsymbol{\alpha} = (\alpha_1, \alpha_2, \dots, \alpha_k)$ the vector of the parameters of the dynamical system. The vector field \mathbf{f} of the system will always be continuous and differentiable with respect to the dynamical variables.

Intermittency phenomenon is characterized by a signal that randomly alternates between regular or laminar phases and sudden, irregular bursts. Experimental observations have shown that the frequency of chaotic bursts increases with an external or control parameter. Basically, Intermittency is the continuous transition between regular and chaotic motion. Intermittency was originally classified into three types called I, II, III. A dynamical system is called intermittent under the condition that its orbits alternate unpredictably between laminar and chaotic phases. These chaotic phases are called bursts and they have a finite duration. The concept of intermittency has been observed in many physical phenomena such as forced nonlinear oscillators, turbulent flows and Lorenz systems.

Definition 1. *The Lorenz system is a system of three nonlinear first-order differential equations, which is extremely useful in fluid mechanics and specifically in the dynamics of heat transfer. The Lorenz system was introduced by Edward Lorenz in 1963 and represents the transition from regular phases to chaos. It has a characteristic property that indicates that it is sensitive to the initial conditions. That is, for small changes in the initial conditions, we can lead to completely different results (known as the butterfly effect). This effect is illustrated in Figure 1.4.*

Intermittency is observed mainly in the phase space of the dynamic system, where by continuously changing the system parameter, the number of equilibrium points and their stability changes. The critical value α_0 , of the parameter, where such a change is observed, is called the bifurcation point.

- i) Type I intermittency is described by the bifurcation of the stability points [25].
 - (a) The first example of the aforementioned bifurcation is the saddle-node bifurcation, where two equilibrium points collide and eradicate each other and disappear. If α_0 , is the critical value, then for $\alpha < \alpha_0$ we have two equilibrium points, one stable node and one unstable saddle. For $\alpha = \alpha_0$ we have a half-stable equilibrium point and finally for $\alpha > \alpha_0$, we do not have any equilibrium point.
 - (b) A Transcritical bifurcation is a local bifurcation, where the equilibrium points change their stability when they collide. For example, if we have two equilibrium points x_1, x_2 and a critical values α_0 then
 - $\alpha < \alpha_0$, $x = x_1$ is stable and $x = x_2$ is unstable.

- $\alpha = \alpha_0$, bifurcation occurs.
 - $\mu > \mu_0$, $x = x_1$ is unstable and $x = x_2$ is stable.
- (c) The third bifurcation is the Pitchfork bifurcation, where one equilibrium point splits into three. The Pitchfork bifurcation is divided into the supercritical case, where the bifurcations Pitchfork branches are stable equilibrium points and the subcritical case, where the bifurcations Pitchfork branches are unstable equilibrium points. More specific for the supercritical case
- $\alpha < \alpha_0$, there exists one stable equilibrium point.
 - $\alpha = \alpha_0$, bifurcation occurs and the equilibrium point becomes unstable.
 - $\alpha > \alpha_0$, two new equilibrium points are created, which are stable and the third remains unstable.

Likewise for the subcritical case:

- $\alpha < \alpha_0$, there exists one unstable equilibrium point.
 - $\alpha = \alpha_0$, bifurcation occurs and the equilibrium point remain unstable.
 - $\alpha > \alpha_0$, two new equilibrium points are created, which are unstable and the third becomes stable.
- ii) Type II intermittency is described by the bifurcation of limit cycles of a dynamical system.

Definition 2. *A limit cycle is a closed trajectory in phase space which spirals into the limit cycle as $t \rightarrow \infty$ (stable cycle) or as $t \rightarrow -\infty$ (unstable cycle) [29].*

Hopf bifurcation is the bifurcation which refers to the local birth or death of a periodic solution from an equilibrium point when a parameter passes its critical value. Hopf bifurcation can be observed in two dimensions or higher. Hopf bifurcation can also be divided into supercritical and subcritical case. Type II intermittency describes a transition from deterministic phases to irregular bursts through the process of period doubling. More specifically, the system initially has a stable equilibrium point and via a supercritical Hopf bifurcation it becomes a stable limit cycle. As the parameter of the system changes, the period of the limit cycle increases from T to $2T$. As a result, two new stable limit cycles are created and the original limit cycle becomes unstable. This process repeats, creating new limit cycle with periods $4T, 8T, 16T$, and so on,

until the system is driven to chaos. One of the most common examples of type II intermittency is the logistic map [5].

- iii) Type III intermittency is the most complicated form. It describes a transition to chaotic phases through a crisis bifurcation. This transition occurs sudden and unpredictable due to a critical instability in a chaotic attractor. More specifically, the system initially has a chaotic attractor and as the system parameter varies, this attractor undergoes a crisis in which his structure changes in an unpredictable manner. Such an example could be the Lorenz system as depicted in Figure 1.4.

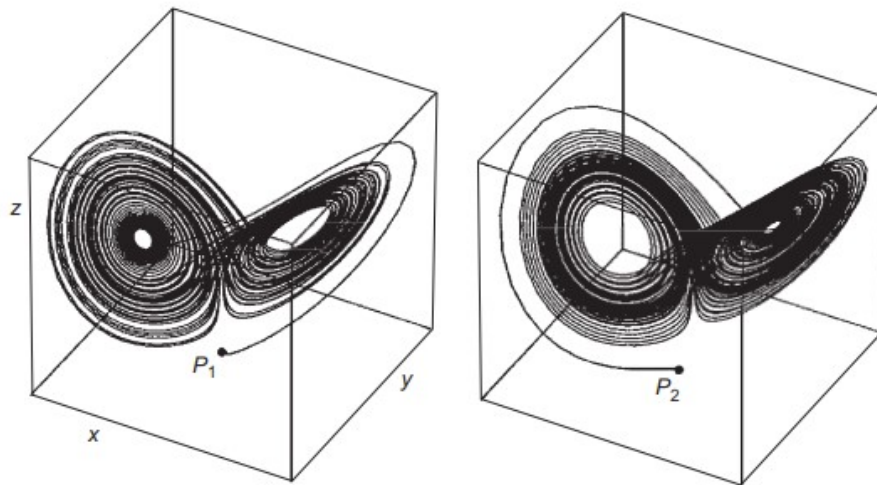


Figure 1.4: Lorenz system showing intermittency. The system spends long periods close to the periodic orbit and suddenly is moving away for phases of chaotic dynamics [10].

CHAPTER 2

MATHEMATICAL BACKGROUND

2.1 Dynamical systems and Phase space

Definition 3. *Dynamical systems are the natural phenomena and physical processes that are interpreted by systems of differential equations of which time is the independent variable.*

The equations that describe such phenomena are non-linear [25]. Dynamic systems are important because they can provide with information about the behavior of the system when time tends to infinity. This is valid at least for the regions where the motion is predictable, whereas area exhibiting chaotic behavior present more complex and uncertain outcomes. Many natural phenomena that we use dynamical systems to study are the weather, the flow of a river, the economy of a country, the relative movements of the planets in a solar system and many others.

If we consider an N -dimensional space of dependent variables $x_k(t), k = 1, \dots, N$ where their independent variable is time t and are components of the vector,

$$\mathbf{x}(t) = (x_1(t), x_2(t), \dots, x_N(t)), \quad t \in I = (a, b)$$

- If t is continuous in the interval I , then the evolution in time is given by the following system of differential equations of first order:

$$\frac{d\mathbf{x}}{dt} = \dot{\mathbf{x}} = f(\mathbf{x}, t) \tag{2.1}$$

- In the other case where t is discrete, the time evolution is described by a system of difference equations (iterative relationships)

$$x_{k,n+1} = g_k(x_n), \quad k = 1, \dots, N \tag{2.2}$$

Definition 4. *The Euclidean space \mathbb{R}^N where the vectors $\mathbf{x}(t)$ and x_n evolve for each instant of time is called the phase space of the system. We can define the position $\mathbf{x}_0 = (x_{1,0}, \dots, x_{N,0})$ at the time t_0 as the initial state of the system.*

Next we define the Van der Pol system:

Definition 5. *The van der Pol equation is an important second-order nonlinear differential equation that has many applications in the study of oscillators with nonlinear damping. The van der Pol equation was introduced by Balthasar van der Pol in 1920 as a model for electrical circuits with nonlinear elements. This equation is very helpful for describing oscillations with a damping form [29].*

The van der Pol equation has been used to describe various natural and artificial systems such as:

1. Electric circuits with non-linear elements
2. Mechanical systems with amplitude dependent damping
3. Biological systems, such as heart activity.

The differential equation is given by the following formula:

$$\frac{d^2x}{dt^2} - \beta(1 - x^2)\frac{dx}{dt} + x = 0.$$

In order to analyze the equation, we convert it into a first-order system.

$$\begin{aligned}\frac{dx}{dt} &= y, \\ \frac{dy}{dt} &= \beta(1 - x^2)y - x.\end{aligned}$$

Depending on the rule of evolution of a dynamic system, it can be classified as either deterministic or stochastic. A system is characterized as deterministic when it always gives the same temporal evolution with a given initial condition. On the other hand, a system is characterized as stochastic when the flow contains some degree of randomness in the evolution rule.

In the continuous case, the system is divided into autonomous or non-autonomous, depending on whether the function $f(\mathbf{x}, t)$ does not explicitly depend on time t or depends on time respectively. For example,

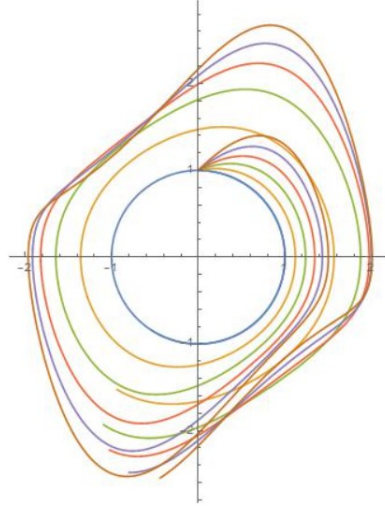


Figure 2.1: Van der Pol oscillator phase space for the different values of the parameter β . The behavior of the oscillator changes significantly as the value β increases, demonstrating non linear dynamics [29].

1. the dynamical system $\frac{dx}{dt} = x(1 - x)$ is autonomous
2. the dynamical system $\frac{dx}{dt} = x - t$ is non-autonomous

The non-autonomous systems are quite complex because the evolution of a point in the phase space depends on the moment in time at which this point is located. It is very important to perform the qualitative analysis of the dynamic systems. At first we have to find and analyze the fixed points of the system. A fixed point known as equilibrium point in a dynamical system is a point where the system does not change. A fixed point also satisfies $f(\mathbf{x}, t) = 0$. A fixed point can be stable or unstable depending on whether the system exhibits attraction or deflection around the point respectively. There also exists the case of a center, that is Lyapunov stable but not asymptotically stable. More specifically, nearby trajectories neither converge nor diverge in comparison to a limit cycle but remain at a constant distance from the fixed point.

In fluid mechanics, equations such as Navier-Stokes can be treated as a dynamic system. The study of turbulent flow can be analyzed through the Burgers equation and Navier-Stokes, which we study as dynamic systems.

2.2 Energy Cascade and Kolmogorov Theory

In order to model the phenomenon of turbulence, energy cascade and the Kolmogorov theory are very important mathematical tools to understand turbulent flow. The turbulent scale provide information about the range of the size over which turbulent structures exist within the flow. These scales can range from large scales (Integral scales) to small scales (Kolmogorov scales) [26]. To be able to adequately study turbulent flow, we must be able to characterize these scales.

A key concept related to turbulent scales is the cascade process, which describes how energy transfers from larger to smaller scales in the turbulent flow. Due to the fact that turbulence is a continuous phenomenon, this transfer occurs across a spectrum. When these eddies interact, the larger eddies break down into smaller ones. This has the consequence of releasing energy that sustains the turbulence into smaller eddies. Turbulence consists of a continuous spectrum of scales which varies from larger to smaller scales. To visualize turbulent flow, we turn the problem into an eddy problem. A defining feature of these eddies is that larger eddies contain many smaller scales and all move together as a structure.

Definition 6. *An eddy is characterized as a local swirling motion, where its turbulent scale defines its characteristic dimension. Eventually, the Kolmogorov eddies dissipate energy as heat due to the effect of the molecular viscosity and as a result entropy is increased. Hence, energy dissipation is always associated with turbulent flow.*

2.2.1 Kolmogorov's scale

Turbulence Kinetic Energy (TKE) is a crucial factor for understanding turbulence. Since small scale motion evolves fast over short time frames, we can assume that such motion is independent of the relatively slow dynamics of larger eddies. As a result, the energy they receive from larger eddies is almost equal to the energy they dissipate as heat. This balance is one of Kolmogorov's assumptions called Universal Equilibrium Theory [23]. Therefore, the motion at the small scales should depend only on two factors:

- The rate at which the larger eddies supply energy ε
- The kinematic viscosity, ν

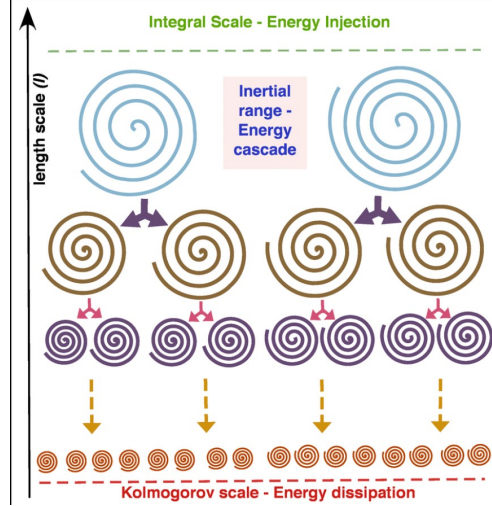


Figure 2.2: The process of energy cascade, large eddies break to small ones.

Definition 7. *Turbulent viscous dissipation per unit mass, which measures the energy loss resulting from the conversion of turbulent kinetic energy into thermal energy within a fluid, is given by the following formula:*

$$\varepsilon = -\frac{dk}{dt}, \quad (2.3)$$

where k is the turbulence kinetic energy, $k = \frac{(u')^2 + (v')^2 + (w')^2}{2}$.

Now introducing ε , which dimensions are $\left[\frac{\text{length}^2}{\text{time}^3}\right]$, and ν , which dimensions are $\left[\frac{\text{m}^2}{\text{s}}\right]$, we are able to form the Kolmogorov scales [22] :

$$\eta \equiv \left(\frac{\nu^3}{\varepsilon}\right)^{\frac{1}{4}}, \quad \text{the Kolmogorov scale length} \quad (2.4)$$

$$\tau \equiv \left(\frac{\nu}{\varepsilon}\right)^{\frac{1}{2}}, \quad \text{the Kolmogorov scale time} \quad (2.5)$$

$$v \equiv (\nu\varepsilon)^{\frac{1}{4}}, \quad \text{the Kolmogorov scale velocity} \quad (2.6)$$

2.2.2 Kolmogorov's -5/3 Law

As previously noted, turbulence encompasses a range of scales, it is convenient for us to approach it through the analysis in terms of the spectrum distribution. This distribution is basically a Fourier-decomposition into wavenumbers κ , or into wavelengths, $\lambda = \frac{2\pi}{\kappa}$. Considering $E(\kappa)$, is the turbulence kinetic energy contained between wavenumbers κ and $\kappa+d\kappa$ applies that:

$$k = \int_0^{\infty} E(\kappa) d\kappa, \quad (2.7)$$

where k the total turbulent kinetic energy [23]. The wavenumbers and scales of the turbulent flow are inversely proportional to each other. That is, for small values of wavenumbers we represent the integral scales while for large values we represent the Kolmogorov scales. Finally, Kolmogorov hypothesized that between the large and small eddies, there is an intermediate state in which the energy cascade is independent of the statistical behavior of the large eddies and of the viscosity. Then we quote Kolmogorov's -5/3 theorem.

Theorem 1. *The Kolmogorov's -5/3 Law is given by:*

$$E(\kappa) = C_k \varepsilon^{\frac{2}{3}} \kappa^{-\frac{5}{3}}, \quad \frac{1}{l} \ll \kappa \ll \frac{1}{\eta}, \quad (2.8)$$

where C_k , is the Kolmogorov constant and κ , is the wavenumber.

In Figure 2.3 we find that the spatial scales are divided into three categories:

- The integral scale where the large eddies contain the largest percentage of energy
- The inertial scale where the eddies have an intermediate scale and the energy spectrum is calculated by Kolmogorov's law as presented in the previous theorem
- The Kolmogorov scale where the Kolmogorov eddies dissipate as heat

2.3 Turbulence Models

Turbulence models play a fundamental role in turbulence modeling, as they are utilized to solve the RANS equations described in Section 4.2. However,

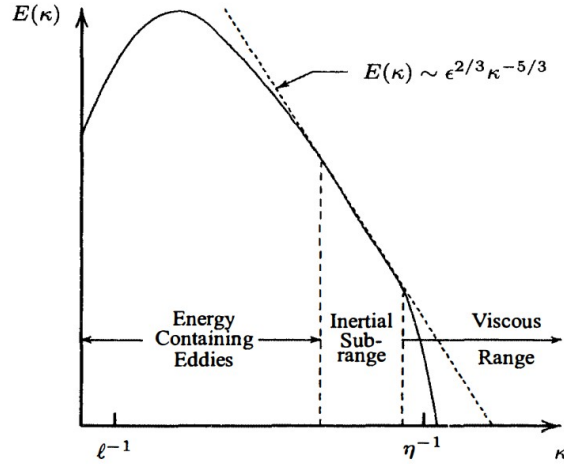


Figure 2.3: Representation of the Energy spectrum of turbulent flow [23].

there is the following problem: the number of unknown parameters is greater than the number of equations. For this reason, we use a turbulence model to solve the problem under consideration evaluating the turbulent kinematic viscosity, ε_t . The first approach is through algebraic turbulence models which articulate the stress tensor components regarding flow variables. The second approach is to add more PDEs in the RANS system. These PDEs calculate the kinematic viscosity as a function of variables such as turbulent kinetic energy (k) or dissipation of energy (ε).

The calculation of turbulent flows, essentially the search for a model for turbulent shear stresses, began by Osborne Reynolds. The absence of advanced computing machines had forced researchers to limit the study of turbulent flows to simple geometries. In the middle of the previous century, a leap forward in computing took place. The development of computers but also the need to study turbulent flow in complex geometries forced scientists to develop several turbulence models to approximate this phenomenon. The most well known are [18]:

1. **Algebraic or zero-equation Models.** These models use algebraic equations which relate the eddy viscosity and some properties of the flow to calculate the Reynolds stress tensor. The main element for these models is Prandtl's theory of mixing length in turbulent flow. Two of the most important models are Cebeci-Smith and Baldwin-Lomax which is a

more advanced version of Cebeci-Smith. The algebraic models were the first to be introduced. However, they have certain limitations such as for example in highly complex flows do not perform well. Algebraic models may not be suitable for laminar to turbulent flow transition applications.

2. **One Equation Models.** These models use a partial differential equation for the turbulent viscosity along with the mean flow equations. These models were created long after algebraic models because their application is limited and is not recommended for complex flows. Therefore, the use of more sophisticated turbulence models is required. Those who first mentioned the weakness of algebraic models and proposed that the turbulent viscosity be described by the differential equation were Kolmogorov and Prandtl. One equation models are more accurate than algebraic ones because they solve an extra partial differential equation. The most popular of them is the Spalart-Allmaras model which was introduced in the early 90s.
3. **Two Equation Models.** Researcher's effort to eliminate the need of calculating the mixing length l , led to the creation of two-equation turbulence models. Two-equation models are among the most well-known and accurate models for the simulation of turbulent flows. These models consist of two partial differential equations that model the turbulent kinematic viscosity. The first equation gives the turbulent kinetic energy and the second gives the diffusion rate of kinetic energy (k - ε) either the specific dissipation rate of the flow (k - ω). The main difference between k - ε and k - ω model is that k - ω is more effective near walls while k - ε performs better in external flow applications. Two-equation models are used as the main tool for CFD for approximately four decades. Compared to the one-equation models, they are quite more efficient because of an additional differential equation. In this thesis we will model the RANS equations through the k - ω turbulence model.
4. **Large eddies simulation-LES.** This method combines the RANS and DNS approach because it uses both the mean flow by RANS and the large eddies formulation. The basic idea behind LES is to reduce the computational cost by ignoring the smallest length scales because are expensive to resolve computationally. The LES model provides excellent accuracy in regions with large eddies.
5. **The DNS method** is a simulation method that solves for all scales of turbulent flow, from integral scales to Kolmogorov scales. The very

important element is that DNS does not need a turbulence model to parameterize the influence of turbulent eddies. More specifically, what it does is solving the Navier-Stokes and give as much detail and accuracy as possible for the fluid flow. However, the DNS method requires extensive computing power as it solves for all scales. So, its use is limited to flows with simple geometries and low Reynolds numbers.

2.3.1 The k - ω Model

Focusing the attention to the one of the most promising turbulence model, the k - ω model. The k - ω model is one of the two-equation models and is used extensively for CFD problems. It describes with great accuracy turbulent flows near walls. The first effort for a k - ω model was proposed by Andrey Kolmogorov in 1942 who introduced the concept of specific dissipation rate in the model [23]. For the following decades many scientists extended his idea with models like Willcox's k - ω model (1988). The most used variation of k - ω models is Menter's SST k - ω model (1994) which combines the advantages of k - ϵ and k - ω models. This model uses k - ω for regions near walls and k - ϵ for the rest of the regions. This property makes it ideal for simulations of complex flows. In this thesis, we will analyze the Willcox's k - ω model. The first

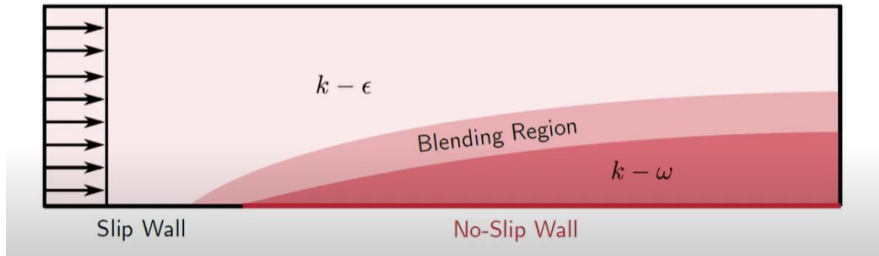


Figure 2.4: Visualization of the SST k - ω model

equation describes the turbulent kinetic energy k , while the second equation describes the specific dissipation rate of the flow, ω . In the k - ω model the turbulent kinematic viscosity is modeled as follows:

$$\varepsilon_t = \frac{k}{\omega}. \quad (2.9)$$

The equations that describe the model are [14]:

1. The partial differential equation for turbulent kinetic energy

$$\frac{\partial k}{\partial t} + u_j \frac{\partial k}{\partial x_j} = \tau_{ij} \frac{\partial u_i}{\partial x_j} - \beta^* k \omega + \frac{\partial}{\partial x_j} \left[(\nu + \sigma^* \varepsilon_t) \frac{\partial k}{\partial x_j} \right] \quad (2.10)$$

2. The partial differential equation for the dissipation rate

$$\frac{\partial \omega}{\partial t} + u_j \frac{\partial \omega}{\partial x_j} = \alpha \frac{\omega}{k} \tau_{ij} \frac{\partial u_i}{\partial x_j} - \beta \omega^2 + \frac{\partial}{\partial x_j} \left[(\nu + \sigma \varepsilon_t) \frac{\partial \omega}{\partial x_j} \right] \quad (2.11)$$

3. The closure coefficients and auxiliary relations:

$$\alpha = \frac{5}{9}, \quad \beta = \frac{3}{40}, \quad \beta^* = \frac{9}{100}, \quad \sigma = \sigma^* = \frac{1}{2}, \quad \varepsilon = \beta^* \omega k \quad (2.12)$$

where :

- $\frac{\partial k}{\partial t}, \frac{\partial \omega}{\partial t}$ are the local derivatives.
- $u_j \frac{\partial k}{\partial x_j}, u_j \frac{\partial \omega}{\partial x_j}$ are the advection terms.
- $\tau_{ij} \frac{\partial u_i}{\partial x_j}, \alpha \tau_{ij} \frac{\omega}{k} \frac{\partial u_i}{\partial x_j}$ are the production terms.
- $\beta^* k \omega, \beta \omega^2$ are the dissipation terms.
- $\frac{\partial}{\partial x_j} \left[(\nu + \sigma^* \varepsilon_t) \frac{\partial k}{\partial x_j} \right], \frac{\partial}{\partial x_j} \left[(\nu + \sigma \varepsilon_t) \frac{\partial \omega}{\partial x_j} \right]$ are the diffusion terms.

One of the advantages of the k - ω model is that, compared to the LES and DNS models, it is less computationally demanding. It is also widely used in flows with intense turbulence, internal flows, aerodynamics. However, it also has some limitations. For example, it does not perform well in free flows.

CHAPTER 3

THE BURGERS' EQUATION

The Burgers' equation is a simplified fluid mechanics model originally proposed by Harry Bateman in 1915 and later studied by Johannes Martinus Burgers in 1948 [13]. The Burgers' equation is an important parabolic partial differential equation that appears in various areas of applied mathematics and physics, such as fluid flow, nonlinear acoustics, gas dynamics and traffic flow. Its viscous form is:

$$\frac{\partial u}{\partial t} + u \frac{\partial u}{\partial x} = \nu \frac{\partial^2 u}{\partial x^2}, \quad (3.1)$$

where $u = u(x, t)$ represents the velocity of the flow and $(x, t) \in \mathbb{R} \times (0, \infty)$ and the kinematic viscosity, $\nu > 0$.

Remark. The kinematic viscosity ν , is a constant physical property of the fluid and the other parameters represent the dynamics that depend on this viscosity.

The Burgers' equation is a simplified version of the incompressible Navier-Stokes equations in a spatial dimension without the pressure term which we consider negligible. Then we will analyze each term of the equation.

- $\frac{\partial u}{\partial t}$ is the velocity rate with respect to time.
- $u \frac{\partial u}{\partial x}$ is the non-linear advection term that represents the velocity transport due to the flow itself and is related to conservation laws.
- $\nu \frac{\partial^2 u}{\partial x^2}$ is the linear diffusion term.

The main goal of this thesis is to examine the balance between the non-linear term and the diffusion term. At first we will mention the inviscid case of the Burgers equation and then we will study its viscous case.

3.1 The inviscid Burgers' Equation

One of the simplest non-linear PDEs is the inviscid Burgers' equation which is of hyperbolic type [28]. It is given by:

$$\begin{cases} u_t + \left(\frac{u^2}{2}\right)_x = 0, & u = u(x, t) \in \mathbb{R}, \quad (x, t) \in \mathbb{R} \times (0, \infty), \\ u(x, 0) = g(x), & (x, t) \in \mathbb{R} \times \{t = 0\}, \end{cases} \quad (3.2)$$

where $g(x)$ is a smooth function. The inviscid Burgers' solution can be given in the form of a traveling wave,

$$u(x, t) = V(x - x_0 - ct), \quad (3.3)$$

with initial condition:

$$u(x, 0) = \begin{cases} u_1, & x \leq x_0, \\ u_2, & x > x_0. \end{cases} \quad (3.4)$$

where $V(y)$ is the step function:

$$V(y) = \begin{cases} u_1, & y \leq 0, \\ u_2, & y > 0. \end{cases} \quad (3.5)$$

This wave could also be called shock wave [28]. With x_0 , we define the point where the shock wave will be located and c is the propagation speed of the wave which is equal to $\frac{u_1 + u_2}{2}$ and will be explained in the next section.

3.1.1 The method of characteristics

We will solve equation (3.2) using the method of characteristics. Let Γ , be a smooth curve on the boundary $\mathbb{R} \times \{t = 0\}$ such that,

$$\Gamma = (x(s), t(s))$$

and

$$z(s) = u(x(s), t(s)),$$

are the values of u , along the curve Γ . By using chain differentiation we have:

$$\frac{dz(s)}{ds} = u_x \frac{dx}{ds} + \frac{dt}{ds}.$$

Comparing that to the initial problem, equation (3.2), we obtain:

$$\begin{cases} \frac{dt}{ds} = 1, & t(r, 0) = 0 \\ \frac{dx}{ds} = z, & x(r, 0) = r \\ \frac{dz}{ds} = 0, & z(r, 0) = g(r) \end{cases}$$

It follows that:

$$\begin{cases} t = s \\ x = g(r)s + r \\ z = g(r) \end{cases}$$

Since u is constant along the curve Γ (from $\frac{dz}{ds} = 0$), we conclude that the characteristics curves are,

$$x = g(r)t + r, \quad (3.6)$$

with $r = r(x, t)$ being the x -intercept of the Γ . Therefore, as far as u is considered,

$$u(x, t) = u(r, 0) = g(r). \quad (3.7)$$

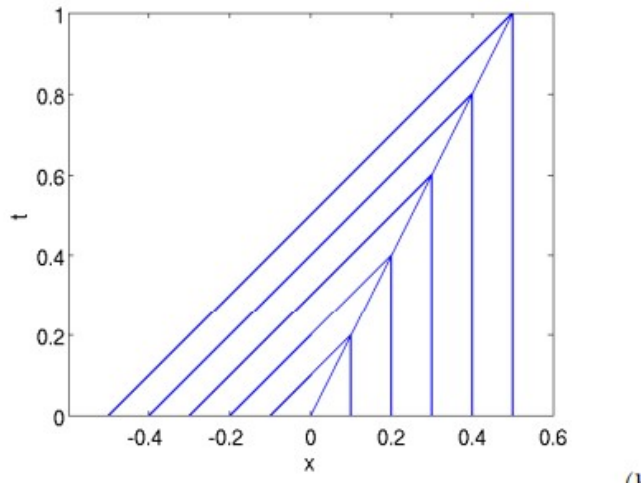


Figure 3.1: Characteristic curves for the inviscid Burgers' equation for $x \in (-0.6, 0.6)$ and $t \in (0, 1)$ [28].

Theorem 2. (*Existence and Uniqueness for the inviscid Burgers' problem*)

The problem equation (3.2) has a unique solution under the condition that g is a C^1 function which satisfies [8]

$$1 + tg'(r) \neq 0. \quad (3.8)$$

The solution is given in the parametric form:

$$\begin{cases} u(x, t) = g(r), \\ x = g(r)t + r \end{cases} \quad (3.9)$$

Proof. Differentiating equation (3.5) and equation (3.6) with respect to x and t we get condition $1 + tg'(r) \neq 0$. Since equation (3.6) also satisfies the initial condition for $t = 0$, because $r = x$, the solution is unique. \square

Remark. So, we conclude that the characteristic curves are straight lines that intersect, a fact that shows the creation of shock waves because an abrupt change is created in the velocity $u(x, t)$, as depicted in Figure 3.1. This happens when $g'(r)$ is negative for a value of r .

3.2 Analytical Solution of the homogeneous Burgers' Equation

In the following section, we will refer to the viscous Burgers' equation (3.1). The Burger's equation can be transformed into an ordinary differential equation (ODE) by the following transformation [3]:

$$\xi = x - ct. \quad (3.10)$$

So, the Burgers' equation transform as follows:

$$\begin{cases} u_t = \frac{\partial u}{\partial \xi} \frac{\partial \xi}{\partial t} = -cu'(\xi) \\ u_x = \frac{\partial u}{\partial \xi} \frac{\partial \xi}{\partial x} = u'(\xi) \\ u_{xx} = u''(\xi) \end{cases}$$

We replace them in equation (3.1) and we have that,

$$-cu'(\xi) + u(\xi)u'(\xi) - \nu u''(\xi) = 0. \quad (3.11)$$

Applying $uu' = \left(\frac{u^2}{2}\right)'$ and integrating equation (3.10), we obtain the following:

$-cu + \frac{u^2}{2} - \nu u' = K$, where K is the integration constant. So, we have the equation

$$2\nu u' = u^2 - 2cu - 2K \quad (3.12)$$

Solving the equation for $u' = 0$, we find two equilibrium points,

$$u_{1,2} = c \pm \sqrt{c^2 + 2K}.$$

The constant c , is equal to the mean value of u_1, u_2 . So, $c = \frac{u_1 + u_2}{2}$ and $K = -\frac{u_1 u_2}{2}$. We arrive at this conclusion with the following procedure.

We set the boundary conditions: $\begin{cases} u(-\infty) = u_1 \\ u(\infty) = u_2 \end{cases}$, assuming $u_1 > u_2$ and $u'(\pm\infty) = 0$. Substituting these conditions we have:

$$-cu_1 + \frac{u_1^2}{2} = K = -cu_2 + \frac{u_2^2}{2}.$$

Therefore, $c = \frac{u_1 + u_2}{2}$ and applying c , in one equation we get $K = -\frac{u_1 u_2}{2}$. So, the final form of the dynamic system can be rewritten as follows:

$$\frac{du}{d\xi} = \frac{(u - u_1)(u - u_2)}{2\nu}. \quad (3.13)$$

Next, we find the analytical solution of the Burgers' equation.

$$\frac{du}{d\xi} = \frac{(u - u_1)(u - u_2)}{2\nu} = f(u).$$

Remark. To analyze the phase space and the equilibrium points, we have to determine whether the derivative of f is positive or negative.

$$f'(u) = \frac{2u - (u_1 + u_2)}{2\nu}. \quad (3.14)$$

Substituting u_1, u_2 into equation (3.13) applies that:

$$\begin{cases} f'(u_1) > 0, & \text{so } u_1 \text{ is an unstable saddle,} \\ f'(u_2) < 0, & \text{so } u_2 \text{ is an stable node.} \end{cases}$$

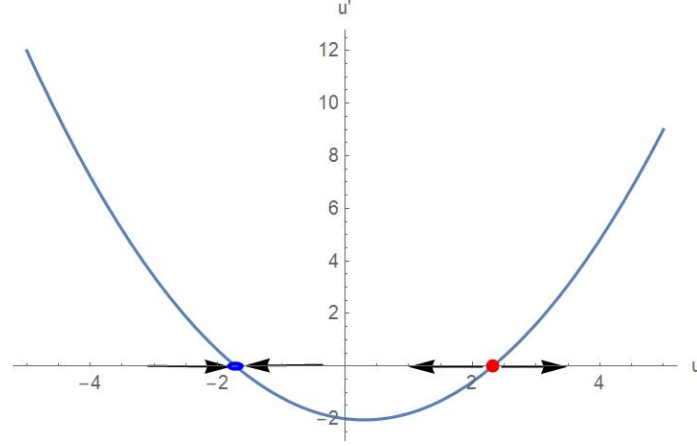


Figure 3.2: Phase space of the Burgers' equation, obtained from the analytical solution.

Remark. From the phase space we conclude that u_1 (red point) is an unstable saddle while u_2 (blue point) is a stable node.

Then we calculate the analytical solution of Burgers' by integrating equation (3.13).

$$\frac{\xi}{2\nu} = \int \frac{du}{(u - u_1)(u - u_2)} \Rightarrow \frac{1}{u_1 - u_2} \ln \left| \frac{u_1 - u}{u - u_2} \right| = \frac{\xi - \delta}{2\nu} \Rightarrow u(\xi) = \frac{u_1 + u_2 e^{\frac{(u_1 - u_2)\xi}{2\nu}}}{1 + e^{\frac{(u_1 - u_2)\xi}{2\nu}}}$$

$$u(\xi) = \frac{(u_1 + u_2)}{2} - \frac{(u_1 - u_2)}{2} \tanh \left(\frac{u_1 - u_2}{4\nu} \left(x - \frac{u_1 + u_2}{2} t \right) \right). \quad (3.15)$$

As we assumed $u_1 > u_2$, the solution $u(\xi)$ decreases monotonically with ξ , we conclude that

$$\begin{cases} \lim_{\xi \rightarrow -\infty} u(\xi) = u_1 \\ \lim_{\xi \rightarrow +\infty} u(\xi) = u_2 \\ u(0) = c = \frac{u_1 + u_2}{2} \end{cases}$$

Remark. The wave occurs at position $x = ct$ ($\xi = 0$) at each time t and propagates linearly in time with constant speed c . We conclude that the smaller the parameter ν becomes, the closer we are to a shock wave behavior. That is, the diffusion term smooths the flow and prevents the creation of shock waves.

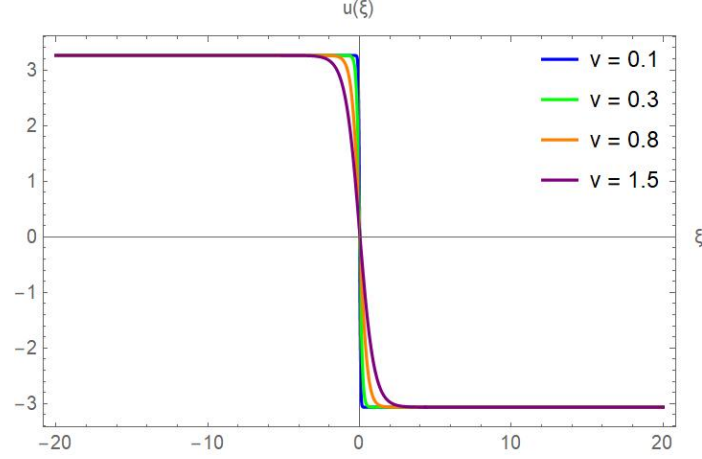


Figure 3.3: Analytical solution of the homogeneous Burgers' equation for different values of ν .

3.2.1 Linearization of the Burgers' Equation

The Cole-Hopf transformation was devised by Eberhard Hopf (1950) and Julian Cole (1951). It is a very important non-linear transformation that transforms the Burgers' equation into the linear diffusion equation [8]. This way, we are able to explicitly solve the non-linear Burgers' equation. Supposing that we have the problem:

$$\begin{cases} \frac{\partial u}{\partial t} + u \frac{\partial u}{\partial x} = \nu \frac{\partial^2 u}{\partial x^2}, & u = u(x, t), \quad (x, t) \in \mathbb{R} \times (0, \infty), \\ u(x, 0) = f(x), & x \in \mathbb{R}. \end{cases} \quad (3.16)$$

We define a function w , as follows:

$$w = \int_0^x u(y, t) dy, \quad w \rightarrow \text{constant as } |x| \rightarrow \infty$$

and

$$h(x) = \int_0^x f(y) dy.$$

So, we have the following Cauchy problem:

$$\begin{cases} w_t + \frac{w_x^2}{2} = \nu w_{xx}, \\ w(x, 0) = h(x). \end{cases} \quad (3.17)$$

We define $v = \varphi(w)$ and choose the function $\varphi(w)$, so that the new equation for v is linear. From the chain rule, we have the following:

$$v_t = \varphi'(w)w_t \text{ and } v_{xx} = \varphi''(w)w_x^2 + \varphi'(w)w_{xx}$$

From the equation (3.16) we apply the term w_t into the term v_t .

$$v_t = \varphi'(w) \left(\nu w_{xx} - \frac{w_x^2}{2} \right) = \nu v_{xx} - \left(\nu \varphi''(w) + \frac{\varphi'(w)}{2} \right) w_x^2 = \nu v_{xx}$$

Supposing that $\nu \varphi''(w) + \frac{\varphi'(w)}{2} = 0$, $\Rightarrow \varphi = e^{-\frac{z}{2\nu}} \Rightarrow v = e^{-\frac{w}{2\nu}} \Rightarrow$

$$w = -2\nu \ln v \quad (3.18)$$

Definition 8. Equation $w = -2\nu \ln v$, is known as the Cole-Hopf transformation.

The function v , as a diffusion equation, has a unique and bounded solution.

$$v(x, t) = \frac{1}{\sqrt{4\pi\nu t}} \int_{-\infty}^{+\infty} e^{-\frac{(x-y)^2}{4\nu t} - \frac{h(y)}{2\nu}} dy. \quad (3.19)$$

So, from equation (3.17) and $w = \int_0^x u(y, t) dy$, we have the final solution of u as follows:

$$u(x, t) = \frac{\int_{-\infty}^{+\infty} \frac{x-y}{t} e^{-\frac{(x-y)^2}{4\nu t} - \frac{h(y)}{2\nu}} dy}{\int_{-\infty}^{+\infty} e^{-\frac{(x-y)^2}{4\nu t} - \frac{h(y)}{2\nu}} dy}. \quad (3.20)$$

3.2.2 Non-homogeneous Case with Forcing Term $f(x, t) = g(x)f(t)$

Consider the forced Burgers' equation,

$$u_t + uu_x = \nu u_{xx} + g(x)f(t). \quad (3.21)$$

Assume a solution of the form:

$$u(x, t) = g(x)a(t) + b(t)w[\xi(x, t), c(t)], \quad \xi(x, t) = g(x)b(t) \quad (3.22)$$

with function w , the solution of the homogeneous Burgers' multiplies by b^3 ,

$$b^3 w_c + b^3 w w_\xi = b^3 \nu w_{\xi\xi}. \quad (3.23)$$

Using the chain rule we can obtain

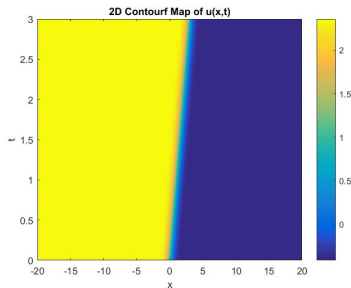
$$\begin{cases} u_t = g\dot{a} + \dot{b}w + bw_\xi g\dot{b} + bw_c\dot{c} \\ u_x = \dot{g}a + b^2w_\xi\dot{g} \\ u_{xx} = \ddot{g}a + b^3w_{\xi\xi}(\dot{g})^2 + b^2w_\xi\ddot{g} \end{cases} \quad (3.24)$$

Substituting (3.23) into equation (3.20) provides with the following system for the functions $a(t)$, $b(t)$, $c(t)$:

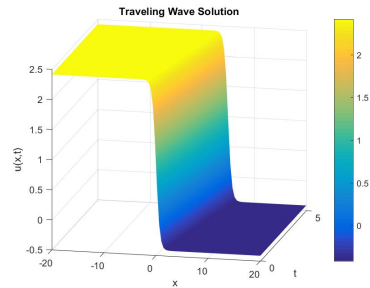
$$\begin{cases} \dot{a} + a^2 = f - \frac{\dot{g}va}{g} \\ \dot{b} + a\dot{g} = 0 \\ \dot{c} = b^2 \end{cases}$$

3.3 Solutions of the Burgers' Equation

In this section we will present the analytical solution of the Burgers' equation. The Burgers' equation could describe the dynamics of shock waves. To implement these results, we use the Matlab program for the representation of the analytical solution. Then we comment on the results and introduce graphical representations.



(a) 2D Burgers' analytical solution.



(b) 3D Burgers' analytical solution.

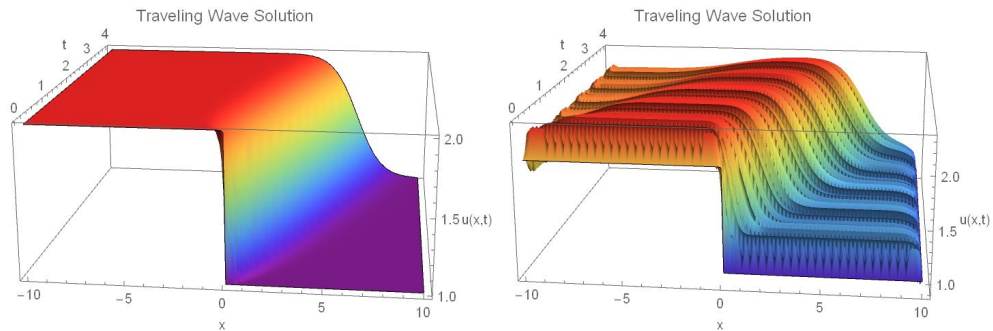
Figure 3.4: Analytical solutions of Burgers equation.

Remark. Figures 3.4 (a), (b) show the analytical solutions of the Burgers' equation as a function of time and space. Of these two graphs, we notice the appearance of waves around the point $x = 0$, where the velocity $u(x, t)$ presents an abrupt change.

In the 3D graphics, we also see that the wave propagates from left to right with increasing time. This time evolution shows that the wave maintains its shape while moving through space. From these results, we understand the usefulness of Burgers' equation on laminar flow. This shows a basis for how changes in the flow field can be studied.

3.3.1 Numerical solution of the non-homogeneous Burgers' equation

In this section we will present the numerical solution of the Burgers' equation for two cases, corresponding to the laminar and turbulent cases. First we will represent the homogeneous (laminar) case and then the non-homogeneous (turbulent) case with the introduction of a sinusoidal term $f(t) = \sin(\omega t)$. For the implementation of these graphics, we will use the Mathematica program.



(a) Numerical solution for homogeneous case. (b) Numerical solution for the non-homogeneous case with a high frequency term, $f(t) = \sin(60t)$.

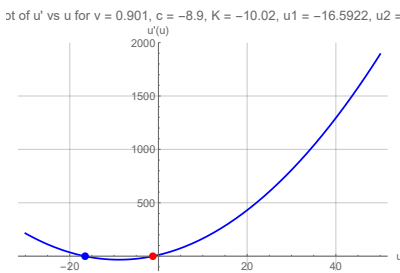
Figure 3.5: Numerical solutions of the Burgers' equation.

The introduction of a sinusoidal term causes a time-varying force that contributes to the appearance and characteristics of the turbulent flow. In Figure 3.5, we observe that the frequency value ω affects the solution presenting fluctuations and leads to a turbulent behavior.

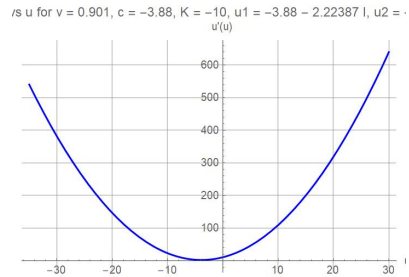
Remark. A very important observation from the graphs is that they maintain the shape of the wave. The sinusoidal function plays a decisive role in the appearance of turbulent behavior in the Burgers equation, with a key element being the frequency ω , where it demonstrates the increase of fluctuations and the final structure of the solution.

3.4 Intermittency in Burgers' Equation

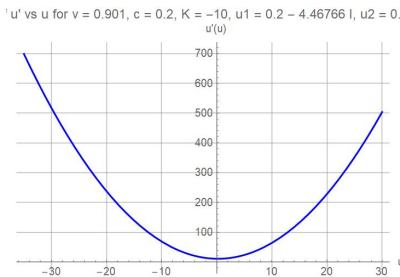
In order to analyze the behavior of the solution of equation (3.12), we focus on the phase space and the equilibrium points of the system at different values of the parameter c , keeping the parameters ν and K fixed. Intermittency is a phenomenon characterized by the alternating between predictable (deterministic) and unpredictable (chaotic) phases. Since Burgers' equation is a (1+1)-dimensional system, involving one spatial and one temporal variable, we cannot observe chaotic behavior due to its low dimensionality. However, the number and stability of the equilibrium points in the phase space determine whether the system exhibits intermittency. Next, we plot the phase space for four different values of c and examine the behavior of the equilibrium points.



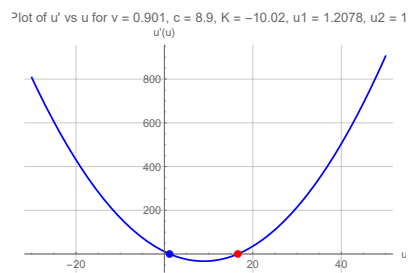
(a) Phase space for $\nu=0.9$, $K=-10$, $c=-9$.



(b) Phase space for $\nu=0.9$, $K=-10$, $c=-3.9$.



(c) Phase space for $\nu=0.9$, $K=-10$, $c=0.3$.



(d) Phase space for $\nu=0.9$, $K=-10$, $c=8.9$.

Figure 3.6: Phase space of the Burgers' equation for different values of the parameter c .

In graph (a), we observe two equilibrium points: an unstable saddle and a stable node. In graph (b), we have one equilibrium point and then in graph (c)

none. Finally in graph (d), two equilibrium points appear again. We observe that the dynamic system presents Type I saddle-node intermittency as the value of the parameter c changes [25].

Remark. This alternating dynamic behavior characterizes Type I saddle-node intermittency.

3.5 Turbulent Burgers' Equation

The one-spatial dimension forced Burgers' equation we consider is:

$$\frac{\partial u}{\partial t} + u \frac{\partial u}{\partial x} = \nu \frac{\partial^2 u}{\partial x^2} + f(x, t). \quad (3.25)$$

The stochastically forced Burgers' equation is one of the most important models for understanding the interaction of random disturbances and the study of turbulent flow [7]. A very important case is adding a term $f(x, t)$ which is a zero-mean Gaussian white-in-time random force, whose Fourier components $\hat{f}(k, t)$ satisfy,

$$\langle \hat{f}(k, t) \hat{f}(k', t') \rangle \sim k^{-\beta} \delta(k + k') \delta(t - t'), \quad (3.26)$$

where k is the wavenumber, $\langle \cdot \rangle$ denotes the time average of a stochastic quantity and δ is the dirac function. From this, we conclude that the energy introduced into the system, depending on the wavenumber, is distributed on different spatial scales. The parameter β shows the excitation we have at each spatial scale. We choose $\beta=1$ since this choice of β yields a K41-type energy spectrum [23],

$$E(k) \sim k^{-\frac{5}{3}}.$$

Definition 9. *The white-in-time force is a stochastic type of external force that has the following properties:*

- It has a zero mean value at different time points, which means that it is statistically symmetric around 0. This can be symbolically expressed as $\langle f(x, t) \rangle = 0$.
- Disturbances are independent at each moment in time, meaning that the disturbances at a moment in time are not affected by the previous ones. That is, there is zero correlation between different time points.

This stochastic force adds energy to all spatial scales which increases the non-linear interaction between the scales. This interaction results in the creation of a shock where the flow is disturbed and becomes more unstable. This is how the phenomenon of dynamic multiscaling appears in the system. This concept defines the situation where non-linear interactions appear on both spatial and temporal scales at the same time. This energy is transferred from large to small scales through the development of Energy Cascade.

Then we define the collision time $tcol(l)$, which is the time interval needed for the fluctuations to start interacting with each other. With the parameter l we denote the mixing length of the flow. The mixing length of the flow represents the characteristic scale of the eddies. More specifically, the longer the mixing length, the larger the eddies in the flow. For eddies with a relatively large scale the collision time $tcol$ is longer, in contrast to the smaller scales where it decreases significantly. This shows that the transition to turbulent flow is enhanced by the fast interactions between the smaller scales.

Turbulent flow is divided into normal and decaying flow [4].

1. In normal turbulent flow, the system receives a continuous supply of energy from external forces. This energy is initially introduced into the eddies with large scales and through the energy cascade is transferred to the smaller scales. Finally, the energy it eventually dissipates through the viscosity molecule and is converted into heat. This continuous input of energy keeps the turbulent flow stable and allows fluctuations to occur.
2. The decaying turbulent flow consists of the flow where there is no more external force to provide energy to the system. So the initial energy that the flow had is gradually exhausted. The fluctuations of the flow decrease with the passage of time and the energy that is transferred to the small scales through the energy cascade, it finally dissipates. As a result, the flow becomes more and more smooth due to the fact that the turbulent state decreases. More details can be found in [4]

CHAPTER 4

NUMERICAL SOLUTIONS OF THE NAVIER-STOKES(N-S) EQUATIONS IN TURBULENT INTERNAL FLOWS

Turbulent internal flows are an important field of research in fluid mechanics because they are applied in many fields such as engineering, water distribution systems, aerospace and biomedical problems such as blood flow in arteries and veins. Turbulent internal flows have the property that near at walls, large changes in the velocity gradient appear. To determine if the internal flow is characterized as turbulent, we use the Reynolds number that defined in previous section. Specifically for flow in a channel, the critical Reynolds number $Re_{\text{critical}} = 2.300$ shows the point at which the transition from laminar to turbulent flow begins to occur. In addition, the critical value at which the flow becomes fully turbulent is $Re_{\text{turbulent}} = 4.000$. One result of turbulent internal flow is that we observe an increase in momentum and in the kinetic energy compared to the laminar flow. In this thesis, we will study the turbulent behavior of a channel of length 10 and height 2. More specifically, it satisfies the no-slip condition on the walls and with a constant computational velocity $u_0 = 5$ m/s at the entrance. We will use a 70×70 grid which was selected from the grid independence study that we perform below.

4.1 Couette and Hagen-Poiseuille flows

In this section, we analyze two of the most important flows in fluid mechanics, which exhibit laminar characteristics but under certain conditions

and certain factors transition into turbulent flow. More specifically, we will discuss about the Couette and Hagen-Poiseuille flows. Initially, we need to define what is a parallel flow.

Definition 10. *Parallel flows represent a simple class of motions. A flow is classified as parallel if only one velocity component remains non-zero and all fluid particles move in one direction [19].*

Assuming that the velocity components v and w are zero, we can conclude from the continuity equation that $\frac{\partial u}{\partial x} \equiv 0$, which articulates that for parallel flows we have,

$$u = u(y, z, t), \quad v \equiv 0, \quad w \equiv 0. \quad (4.1)$$

In addition, it also follows that $\frac{\partial P}{\partial y} = \frac{\partial P}{\partial z} = 0$ and the Navier-Stokes equations appear in the following form:

$$\rho \frac{\partial u}{\partial t} = -\frac{\partial P}{\partial x} + \mu \left(\frac{\partial^2 u}{\partial y^2} + \frac{\partial^2 u}{\partial z^2} \right). \quad (4.2)$$

4.1.1 Couette flow

Couette flow is a fundamental and well studied case. It describes the flow of a fluid between two parallel flat walls, one of which is at rest and the other is moving with a constant velocity U . Couette flow is important for the study of shear forces and the viscous nature of the fluid. It is a steady flow and the velocity component u , depends only on the y -direction. So, equation (4.2) can be rewritten as,

$$\frac{\partial P}{\partial x} = \mu \frac{\partial^2 u}{\partial y^2}. \quad (4.3)$$

Considering the boundary conditions:

$$\begin{aligned} y = -h : u &= 0, \\ y = h : u &= U. \end{aligned}$$

we obtain the solution [24]:

$$u = \frac{U}{2} \left(1 + \frac{y}{h} \right) - \frac{1}{2\mu} \frac{\partial P}{\partial x} (h^2 - y^2). \quad (4.4)$$

By solving for the flow rate:

$$Q = \int_{-h}^h u(y) dy,$$

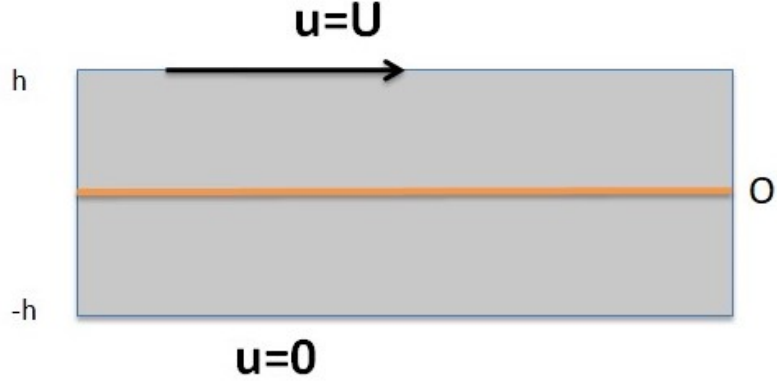


Figure 4.1: Couette flow in a channel

we can define that,

$$\frac{\partial P}{\partial x} = -\frac{3\mu}{2h^3}(Q - Uh). \quad (4.5)$$

For the case of zero pressure gradient, the flow is referred to as simple Couette flow and it is given by:

$$u = \frac{U}{2} \left(1 + \frac{y}{h} \right) \quad (4.6)$$

and the shear stress is uniform across the flow field and it is given by Newton's law of viscosity:

$$\tau = \mu \frac{U}{h}. \quad (4.7)$$

In Couette flow, there are three different cases concerning the pressure gradient. The first case occurs when the pressure gradient is zero and the velocity profile is given by equation (4.6). The second case arises when there is negative pressure gradient which is called favorable and the velocity is given by equation (4.4). The third case, which is the most interesting, involves a positive pressure gradient which is called adverse and it means that the pressure increases across the flow field. In Figure 4.2, by using the program Mathematica, we represent the graphical representations for the three different cases of the pressure gradient.

Transition to turbulence in Couette flow.

The transition from laminar to turbulent Couette flow is considered a defining problem in fluid mechanics, because it provides information about non-linear

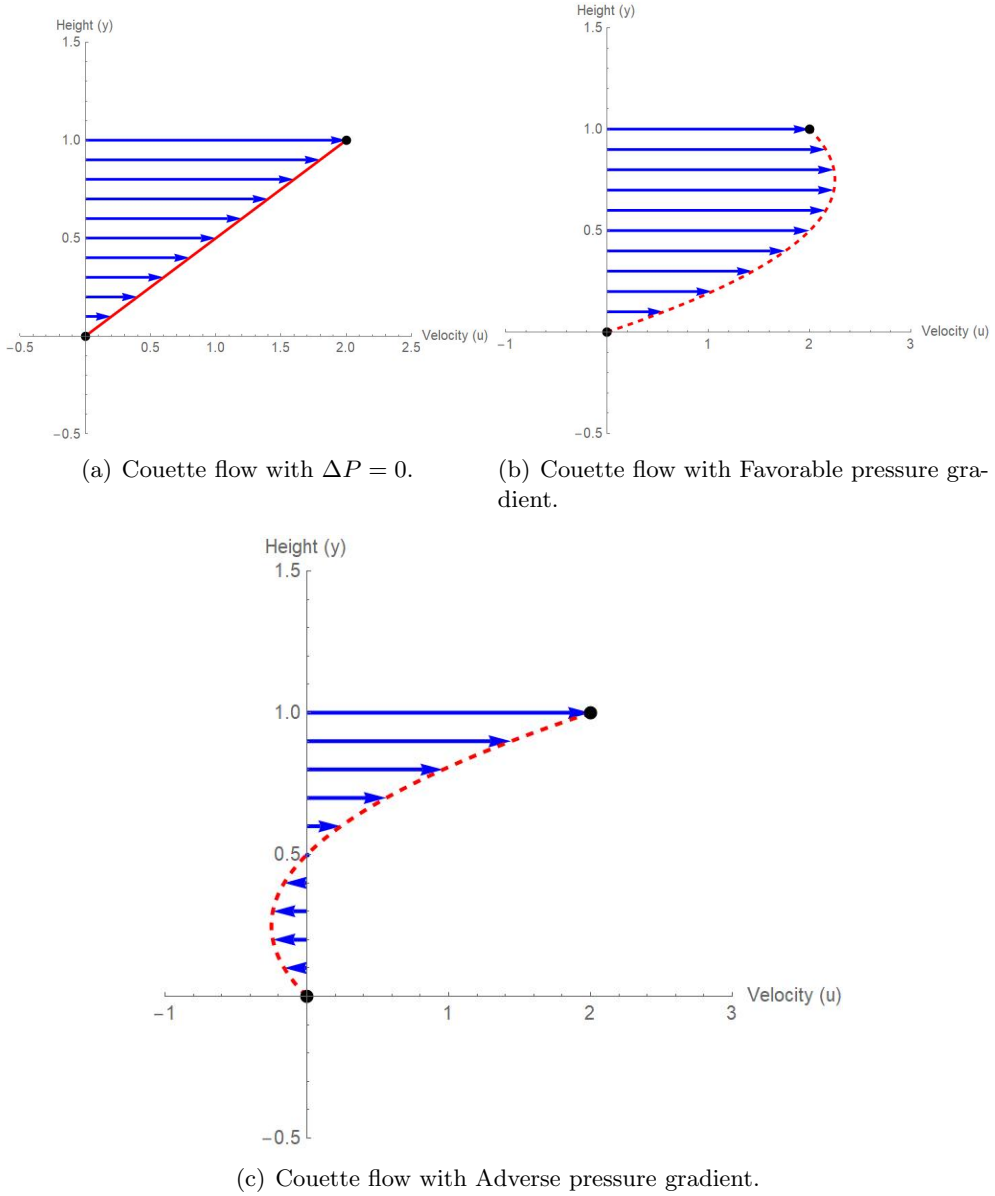


Figure 4.2: The three different cases for the pressure gradient.

dynamics and flow stability. Couette flow is linearly stable at all Reynolds numbers. However, it has been shown that for $Re > 1,000$, turbulence is usually observed under specific conditions.

The “**bypass**” transition mechanism describes the appearance of turbulence in flows such as Couette flow, where linear instabilities are absent. More specifically, external or internal disturbances with sufficient intensity, bypass the stable laminar state. These disturbances are the main reason why the so-called “**streaks**” appear [15]. They are referred as localized regions of increased or decreased velocity. The destabilization of these “streaks”, often cause turbulence. This process is known as the lift-up effect. As a result, there occurs non-linear interactions that make the phenomenon of turbulence to appear. This particular mechanism is important at higher values of Reynolds numbers, because local turbulent regions develop through secondary instabilities, which destabilize the “streaks” even more. In Couette flow the transition is characterized by spatiotemporal intermittency where the laminar regimes alternate with turbulent ones over space and time, contributing to better understanding of turbulence onset in stable flows [15].

4.1.2 Hagen-Poiseuille flow

The Hagen-Poiseuille flow is a flow that analyzes the steady, laminar flow of a viscous, incompressible fluid through a cylindrical channel. It describes the pressure drop due to the fluid viscosity. The flow is laminar through a channel of constant circular cross-section that is substantially longer than its diameter and there is no acceleration of the fluid. For velocities and channel diameters that surpass a critical value, the flow becomes turbulent and as a result it leads to larger pressure drop compared to the laminar case. The velocity profile of Hagen-Poiseuille flow is parabolic and it is given in cylindrical coordinates by the following formula [17].

$$u(r) = \frac{\Delta P}{4\mu L} (R^2 - r^2), \quad (4.8)$$

where:

- ΔP the pressure difference
- μ the dynamic viscosity
- L the length of the pipe
- R the pipe radius
- r the distance from the central axis of the pipe

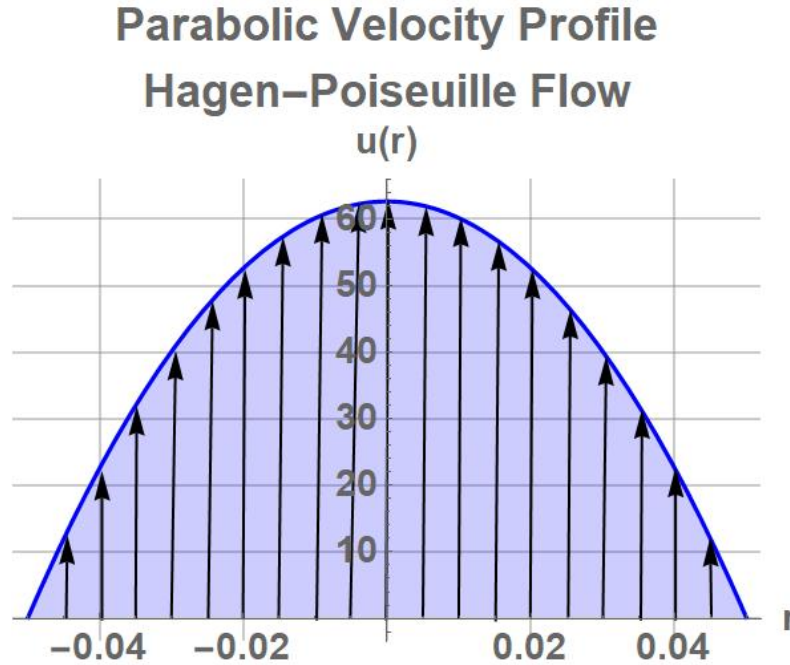


Figure 4.3: The velocity profile of the Hagen-Poiseuille flow

The velocity profile satisfies the no-slip condition at the walls and its maximum value is at the center of the channel ($r=0$). In Figure 4.3, we represent the parabolic profile of the velocity u . The pressure drop is given by:

$$\Delta P = \frac{8\mu LQ}{\pi R^4}, \quad \text{where } Q \text{ is the flow rate.}$$

The energy dissipated as heat due to the viscous effects is calculated as:

$$P_{loss} = Q\Delta P.$$

For turbulent flow the pressure drop can be found from the Darcy–Weisbach equation [17]:

$$\Delta P = \Lambda \frac{L}{D} \frac{\rho u^2}{2}, \quad (4.9)$$

where:

- L the length of pipe
- ρ the density of fluid

- D the diameter of pipe
- u the mean velocity
- Λ the Darcy friction factor

Definition 11. *In fluid mechanics, the Darcy friction factor is a dimensionless quantity which is used to measure the frictional resistance caused by the fluid flow. This quantity affects the pressure drop and it is directly connected with the Reynolds number and the wall roughness.*

The Darcy friction factor applies to both laminar and turbulent flow.

1. For laminar flow ($Re < 2.000$), the Darcy friction factor is $\Lambda = \frac{64}{Re}$
2. For turbulent flow, the Darcy friction factor can be calculated through empirical formulas such as the Colebrook-White equation [11]:

$$\frac{1}{\sqrt{\Lambda}} = -2 \log_{10} \left(\frac{\gamma}{3.7D} + \frac{2.51}{Re\sqrt{\Lambda}} \right), \text{ where } \gamma \text{ is the wall roughness}$$

Additionally, there is the Blasius approximation which says that for smooth channels and $4.000 < Re < 100.000$ then it holds that [11]:

$$\Lambda = 0.316 Re^{-0.25}$$

Transition to turbulence in Hagen-Poiseuille flow.

The transition of Hagen-Poiseuille flow from laminar to turbulent flow is a critical phenomenon in fluid mechanics. The most important factor that affects the transition is the Reynolds number but there are some external and internal factors that also contribute to the transition [19]. First, the surface roughness of the channel walls is extremely important because for smooth channels the transition occurs at Reynolds number close to 4.000. On the contrary, for rough channels transition occurs at lower Re due to some irregularities causing turbulence. In addition, the initial state of the flow is a defining factor, because for initial state with disturbances, the transition occurs for $Re < 2.000$. The dynamic viscosity also enhances the viscous terms of the flow, preventing the inertial forces to overcome the viscous ones, leading to turbulence. Finally, the geometry of the channel is crucial because for longer or curved channels it is more likely turbulence to occur.

4.2 Turbulent Channel flow with k - ω model

In this section, we will study the incompressible, steady-state, two-dimensional turbulent channel which is described by the Reynolds Average Navier Stokes (RANS) equations. The RANS equations and the k - ω equations, in closed form, are:

$$\frac{\partial u}{\partial x} + \frac{\partial v}{\partial y} = 0, \quad (4.10)$$

$$\frac{\partial u^2}{\partial x} + \frac{\partial(uv)}{\partial y} = -\frac{1}{\rho} \frac{\partial p}{\partial x} + \frac{\partial}{\partial x} \left[(\nu + \varepsilon_t) \frac{\partial u}{\partial x} \right] + \frac{\partial}{\partial y} \left[(\nu + \varepsilon_t) \frac{\partial u}{\partial y} \right], \quad (4.11)$$

$$\frac{\partial v^2}{\partial y} + \frac{\partial(uv)}{\partial x} = -\frac{1}{\rho} \frac{\partial p}{\partial y} + \frac{\partial}{\partial x} \left[(\nu + \varepsilon_t) \frac{\partial v}{\partial x} \right] + \frac{\partial}{\partial y} \left[(\nu + \varepsilon_t) \frac{\partial v}{\partial y} \right], \quad (4.12)$$

$$\frac{\partial(uk)}{\partial x} + \frac{\partial(vk)}{\partial y} = \frac{k}{\omega} \left(\frac{\partial u}{\partial y} + \frac{\partial v}{\partial x} \right)^2 - \beta^* k \omega + \frac{\partial}{\partial x} \left[(\nu + \sigma^* \varepsilon_t) \frac{\partial k}{\partial x} \right] + \frac{\partial}{\partial y} \left[(\nu + \sigma^* \varepsilon_t) \frac{\partial k}{\partial y} \right], \quad (4.13)$$

$$\frac{\partial(u\omega)}{\partial x} + \frac{\partial(v\omega)}{\partial y} = \alpha \left(\frac{\partial u}{\partial y} + \frac{\partial v}{\partial x} \right)^2 - \beta \omega^2 + \frac{\partial}{\partial x} \left[(\nu + \sigma \varepsilon_t) \frac{\partial \omega}{\partial x} \right] + \frac{\partial}{\partial y} \left[(\nu + \sigma \varepsilon_t) \frac{\partial \omega}{\partial y} \right], \quad (4.14)$$

with the following boundary conditions:

$$\begin{aligned} y = 0 \quad \text{and} \quad y = h : u = v = k = 0, \quad \omega = c, \quad \text{where } c \text{ is a constant.} \\ x = L : p = 0. \end{aligned}$$

With the help of FVM described below, we transform the RANS equations and the k - ω equations into their discrete form. The Appendix provides the entire procedure for converting the equations into their discrete form and a detailed explanation of the conversion of the k - ω model equations to their closed form.

4.3 The Finite Volume Method (FVM)

Computational Fluid Dynamics (CFD) is a numerical simulation tool that has become crucial for the development of a wide range of technologies. The

Finite Volume Method (FVM) is a Discretization technique with second-order accuracy (its simplest form) that is used to solve Partial Differential Equations (PDEs). More specifically, this method transforms the PDEs which represent conservation laws into a system of discrete algebraic equations. This occurs by integrating the PDEs over each discrete control volume.

In FVM, the first step is to discretize the computation domain into non-overlapping finite volumes [16]. These volumes surround a node, where the dependent variables are obtained. Each of these control volumes often calculate the variables at their center.

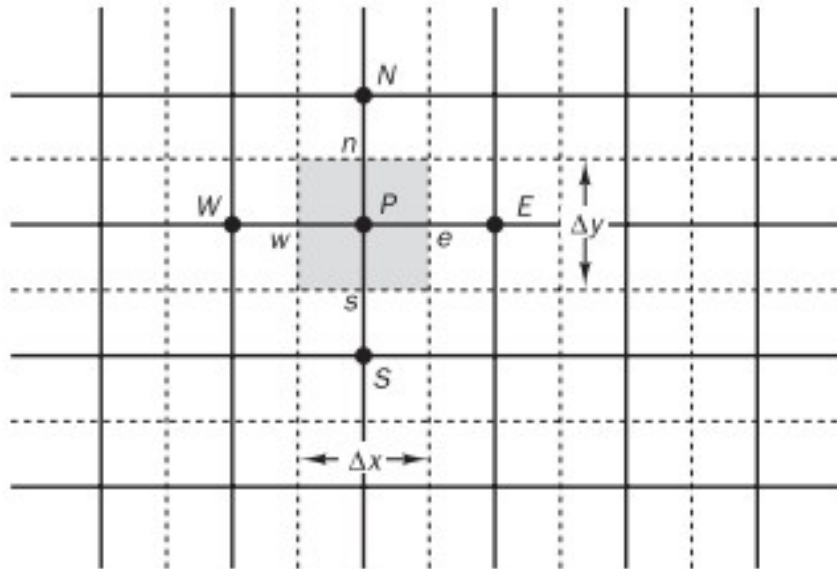


Figure 4.4: Mesh representation for the FVM with Δx and Δy [22].

In the FVM, specific terms in the conservation equations are converted into face fluxes and are evaluated at the finite volume faces. Because the flux entering a control volume is the identical to that leaving, the FVM is conservative and divergence-free. So, the FVM is ideal for CFD problems and for simulations with complex geometries or turbulent flows. In addition, it is easy to implement a variety of boundary conditions because the dependent variables are calculated at the center of the control volume.

The second step is to integrate each term in the PDEs over the control volumes. We calculate the fluxes across the faces of control volumes. Fluxes provide information about the rate at which quantities move across boundaries [22]. We can calculate these fluxes by using Central Differencing, Upwind Differencing or Higher-Order Schemes. Then we use an direct solver to solve

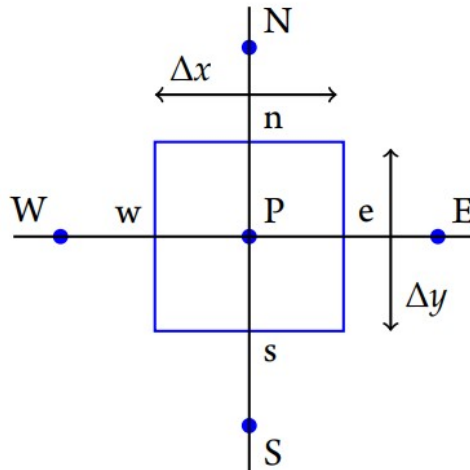


Figure 4.5: Representation of the control volume with a central node P surrounded by: north (N), south (S), east (E), west (W) node.

the resulting algebraic system of equations. For unsteady flows we can use time-stepping methods such as the backward Euler method [9]. Finally, we apply the boundary conditions at the control volume along the computational domain's edges. Two of the most widely used ones are the Dirichlet and the Neumann boundary conditions. In this thesis we apply the FVM to discretize the unsteady Reynolds average Navier-Stokes equations (URANS) for the numerical solution of turbulent channel flow.

Computational Mesh of turbulent channel

In order to be able to represent the turbulent boundary layers, we apply a graded mesh on the channel walls in the y -direction. In the x -direction, the mesh is uniform. In this thesis, we use a 70×70 grid because it produces the best results as we will demonstrate in grid independence study. To generate a graded mesh in y -direction, we apply the hyperbolic tangent function as a common technique for stretched structured grids [21]. Otherwise, the variant

is described as follows:

$$c = \frac{2i - J - 3}{J - 1}, \quad y_i = \left[\frac{1 + \tanh(K \cdot c)}{K_1} \cdot \frac{M}{2} \right], \quad i = 1, 2, \dots, J, \quad (4.15)$$

where $K = 1.8$, $K_1 = \tanh(K)$, $J =$ number of nodes in y -direction (4.16)

More specifically, J is the number of points in the y -direction, M is the height of the pipe, and K is the stretch rate. The stretch rate determines how dense the mesh is near the walls. In turbulent flow, the gradient of the velocity is large and their profiles are steep. As a result, a graded mesh is highly recommended.

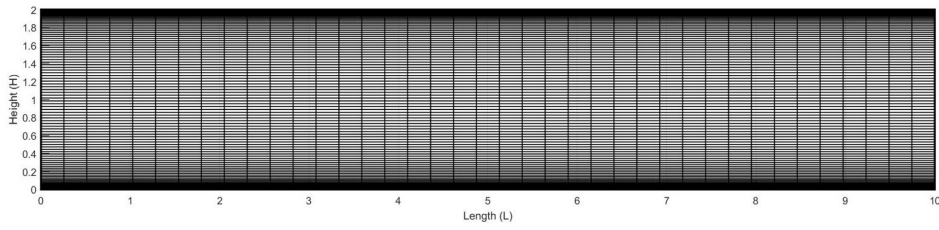


Figure 4.6: Graded mesh for turbulent channel flow, with higher density near walls.

Error estimation: The Root Mean Square

The Root Mean Square (RMS) value of a matrix is the scalar quantity that is described by the following equation:

$$\text{RMS} = \sqrt{\frac{1}{(K+2)(J+2)} \sum_{i=0}^{K+1} \sum_{j=0}^{J+1} x(i,j)^2}, \quad (4.17)$$

where $x(i, j)$ are the elements of the matrix. The RMS provides a measure of the magnitude. This metric is used in the grid independence study to evaluate the percentage differences between various grids. It is very important to determine the optimal computational grid, because it is our purpose to minimize the computational cost with the most accurate numerical solution.

Grid independence study

As mentioned, in a CFD code we need to minimize the computational cost which is done through the grid independence study. We consider a 80×80 reference grid and calculate the percentage differences, requiring them to be smaller than 2 %. These percentage differences can be found through RMS and more specifically through the following equation:

$$\text{Error} = \left(\frac{\text{RMS}_{i \times i} - \text{RMS}_{80 \times 80}}{\text{RMS}_{80 \times 80}} \right) \times 100\%, \quad i = 30, 40, 50, 60, 70. \quad (4.18)$$

Grid Size	u-velocity(%)	v-velocity(%)	pressure(%)
30×30-80×80	1,51	7,04	7,09
40×40-80×80	0,92	4,22	4,77
50×50-80×80	0,55	2,81	3,61
60×60-80×80	0,36	1,40	3,03
70×70-80×80	0,13	0,01	1,59

Table 4.1: Percentage Changes in Turbulent.

Remark. Table 4.1 presents the percentage errors across all grid sizes compared to 80×80 grid. According to the table, we conclude that the optimal grid size is 70×70 because the percentage differences in each individual quantity is smaller than 2%.

4.3.1 Results in Turbulent Channel

In this section, we will present the numerical results for the turbulent channel for a 70×70 grid and compare them to the laminar case. From the expression $Re = \frac{u\rho M}{\mu}$, we conclude that the Reynolds number Re is 10.000.

At the entrance of the channel, the flow is not fully developed, which means that the fluid accelerates or decelerates. At the inlet, the pressure gradient is much greater because the flow is not fully developed, while in the field of fully developed flow, the pressure decreases linearly. We therefore conclude that for fluid flow to occur, the pressure gradient must overcome the viscous forces which resist to the motion of the fluid.

Then we analyze the main differences between laminar and turbulent flow and we establish them graphically. In laminar flow the shear stresses are

given by the experimental Newton's law. However, this is not the case in turbulent flow, because by substituting the velocity with its mean value and its fluctuating value, according to Boussinesq hypothesis the shear stresses are much larger. This happens because the packages of fluid particles (eddies) are moving together, as one structure. These additional stresses are called eddy viscosity stresses [23].

A characteristic difference between the turbulent and laminar flow is their velocity profiles. More specifically, the intense mixing in turbulent flow causes large velocity fluctuations and as a result enhanced momentum transfer. Therefore, a steeper velocity profile is created as it is observed in Figure 4.7.

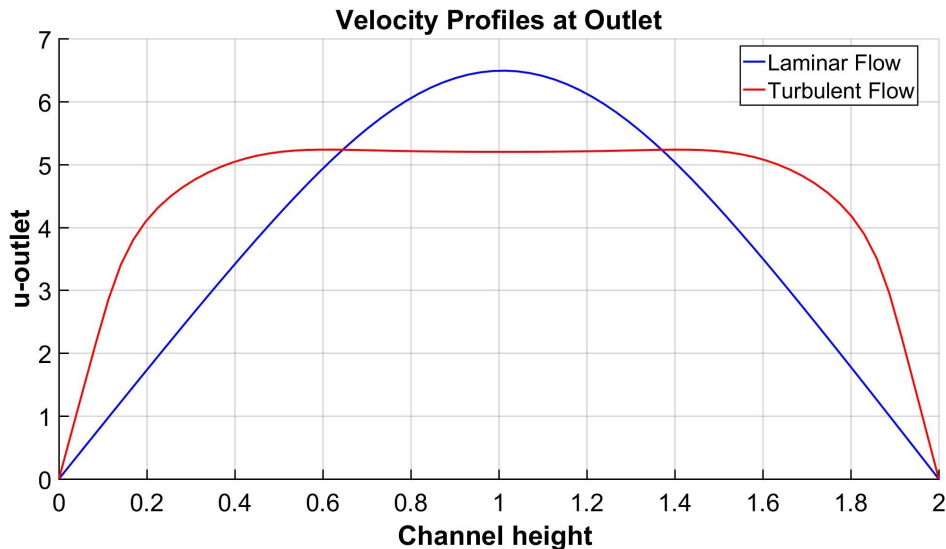


Figure 4.7: Comparison of outlet velocity profiles in laminar case (blue) and turbulent case (red).

Remark. The boundary layer in turbulent flow is thinner due to the enhanced momentum transfer and increased mixing compared to laminar flow, driven by the turbulent eddies. In combination with the no slip condition that applies to the walls, a steeper velocity profile is created compared to the laminar flow, as shown in Figure 4.8.

In the viscous sublayer of the boundary layer, the laminar stresses dominate and we consider negligible eddy viscosity stresses. In the overlap, both laminar and turbulent stresses contribute to the overall stress distribution. In the outer layer, turbulent stresses dominate and they are greater than the laminar ones.

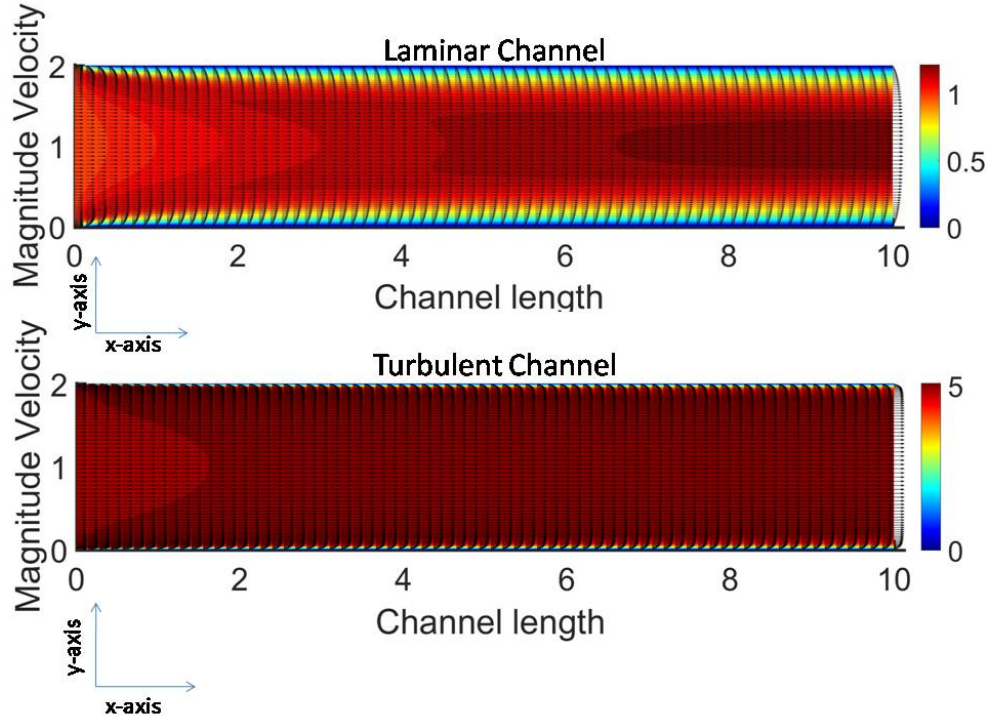


Figure 4.8: Magnitude of velocity in laminar and turbulent channel.

In Figures 4.9, we observe that in turbulent case, pressure has higher values than in laminar case. In turbulent flow, greater shear stresses arise and increase the total shear stresses at the wall. To sustain fluid flow, a greater pressure gradient is required to overcome the viscous forces which have been increased due to the Reynolds stresses.

In Figures 4.10, we present the stresses at the wall for both laminar and turbulent flow. The x -axis represent the channel length and the y -axis shows the stresses at the wall.

Remark. At the entrance of the channel the stresses take their maximum value due to the abrupt change of the boundary layer. Afterwards, as the flow stabilizes, the stresses gradually decrease. It has been shown experimentally that the maximum value in the turbulent flow increases by 25% compared to the laminar flow, which can also be seen in the graphical representations where the maximum value increases from 0.16 to 0.19, as shown in Figure 4.10.

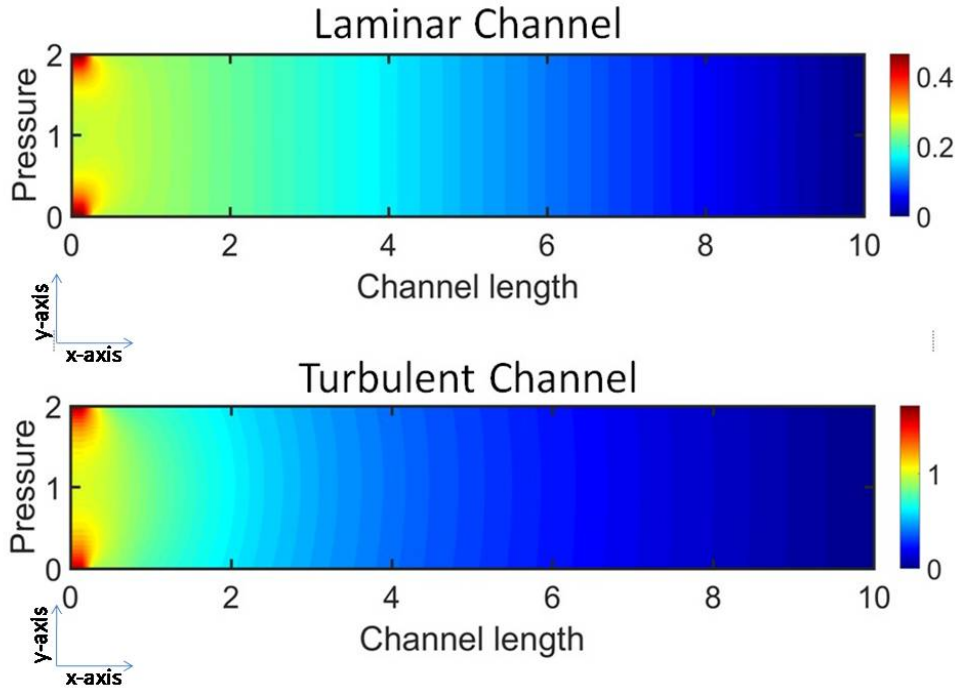


Figure 4.9: Pressure Distribution in laminar and turbulent channel.

In Figure 4.11, we present the eddy viscosity contours, which illustrate the spatial distribution of turbulence intensity. The eddy viscosity is computed as $\nu_t = \frac{k}{\omega}$, where k, ω from the $k - \omega$ turbulence model.

Remark. The largest values of the eddy viscosity are observed at the entrance of the channel where the shear stresses and production volumes dominate. As the flow develops, we observe a decrease in the eddy viscosity with the smallest values being in the center of the pipe and on the walls, where we have a large contribution of ω .

4.4 Solving the unsteady turbulent Navier-Stokes (URANS)

In this section, we study the incompressible, unsteady ($\frac{\partial q}{\partial t} \neq 0$), two dimensional turbulent channel which is governed by the URANS equations. The

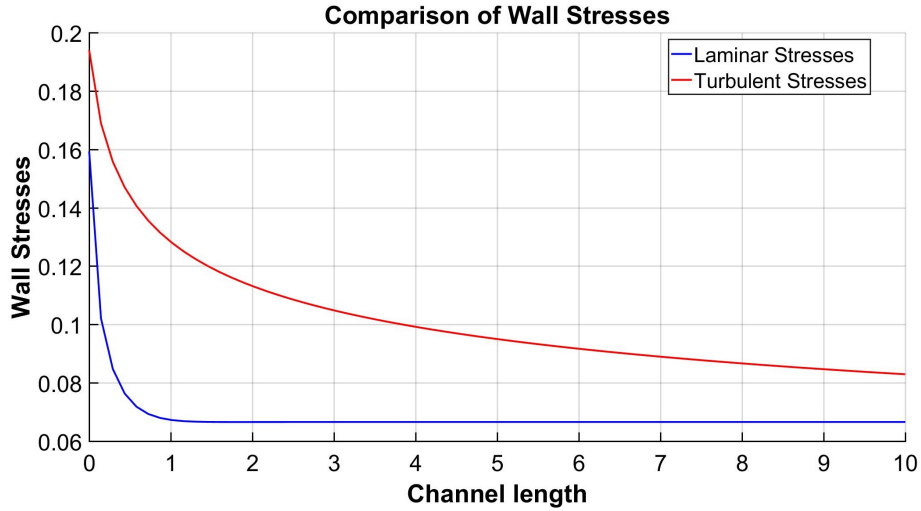


Figure 4.10: Comparison of stresses in laminar and turbulent channel.

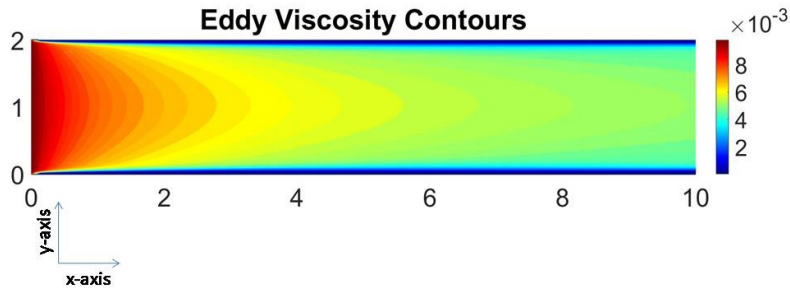


Figure 4.11: Eddy viscosity distribution along the channel.

URANS equations along with the time-dependent equations of the $k-\omega$ model, are described by the equations (4.10)-(4.14) with the inclusion of the time dependent term. The discretization of the equations can be found in the Appendix. This section is important because with the time-dependent equations we can study the phenomenon of intermittency. More specifically, the transition from laminar to turbulent flow and vice versa.

4.4.1 CFL Criterion

Before proceeding to the numerical results obtained, we first point out an important stability criterion, which is the CFL (Courant-Friedrichs-Lewy) number [12]. It is a dimensionless number, which is used for the numerical solution of hyperbolic and parabolic partial differential equations. More specifically, it is a criterion that indicates the numerical stability of a solution and limits the time step that we can apply for a given spatial discretization [12].

The CFL number is given by the following expression:

$$\text{CFL} = \frac{U\Delta t}{\Delta x},$$

where

- U : the characteristic velocity of the flow
- Δt : the time step of the simulation
- Δx : the spatial grid spacing

More generally, in higher dimensions, the CFL number is given by the following relation:

$$\text{CFL} = \sum_{i=1}^n \frac{U_i \Delta t}{\Delta x_i}.$$

To ensure the stability of the solution, we must keep the CFL number below a specific threshold which varies in different cases based on the numerical approach. In this thesis, the following condition will be satisfied [20]:

$$\text{CFL} \leq 1$$

If the CFL is greater than 1 then the solution is characterized as numerically unstable, if the numerical method is explicit. To keep the CFL number small, we can introduce very small time steps in the simulation, but then the computational cost will increase. Therefore, the value of 1 helps to determine the optimal time step for a given characteristic speed and spatial step.

4.4.2 Numerical results

In this section, we present the numerical results for the unsteady turbulent channel case. Considering an initial velocity $u_0 = 0.5$ m/s, from the expression

$Re = \frac{u\rho M}{\mu}$, we conclude that the Reynolds number $Re = 100$. Careful consideration must be given to the time and space discretization so that the CFL stability criterion is satisfied. The main objective of this thesis is to demonstrate that the time-dependent flow under suitable boundary conditions can transition the flow from laminar to turbulent and, under specific conditions, return to the laminar regime. Below we present five time frames from the simulation for different time instances.

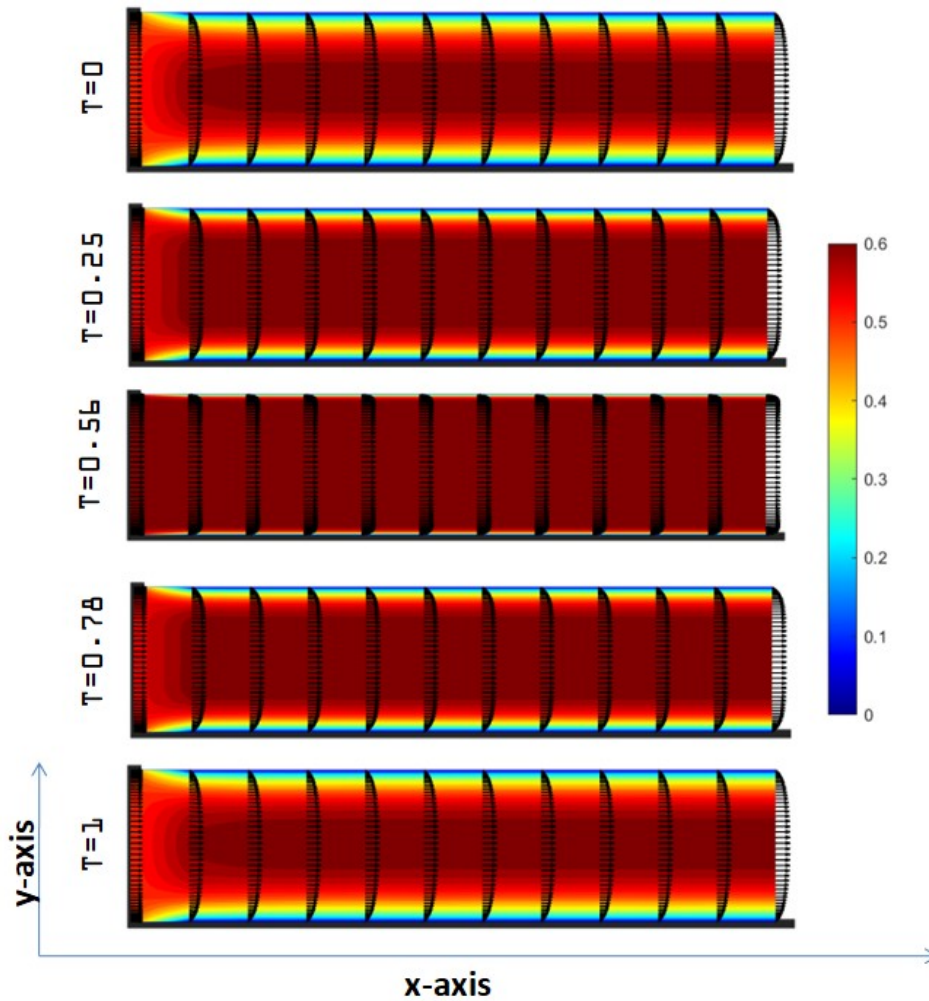


Figure 4.12: Visualization of the magnitude distribution at various time instances, where x -axis represent the channel length and y -axis represent the channel height.

Figure 4.12 illustrates the phenomenon of intermittency using a numerical approach and solving the URANS equations. Initially, the flow starts at $T=0$ from a laminar state and after $T=0.56$ it transitions into a turbulent flow which is evident from the fact that the velocity profile becomes steeper and the thickness of the boundary layer decreases noticeably. Eventually, under specific conditions, at $T=1$ the flow reverts to a laminar state. These transitions are critical for understanding the onset of intermittency. Summarizing, Figure 4.12 numerically confirms that the time-dependent nature of the flow contributes to the appearance of intermittency, where continuous alternations between stable (laminar) and chaotic (turbulent) flow occur.

CHAPTER 5

CONCLUSIONS

In this concluding chapter, we summarize all the essential aspects of the thesis.

Chapter 1:

- Introduction to laminar and turbulent flow
- Analysis of the transition from laminar to turbulent flow
- Introduction to the intermittency phenomenon
- Phase space analysis and how it interprets the state of transient phenomena, such as intermittency

Chapter 2:

- Definition of dynamical systems and further analysis of the phase space
- Overview of Kolmogorov's theory and definition of the concept of energy cascade in turbulent flow
- Review of all turbulence models. Analysis of the k - ω model which we used for the numerical study of turbulent flow

Chapter 3:

- Theoretical analysis of the Burgers' equation cases with respect to important properties
- Reference to the fact that the Burgers' equation is one of the main tools for the study of turbulent flow

Chapter

- The numerical solution of the Burgers' equation, resulting in the structure of waves, contributes to the study of intermittency

Chapter 4:

- Introduction to internal flows such as Couette and Hagen-Poiseuille flow
- Introduction of the finite volume method (FVM) for the numerical solution of the given equations of fluid flow
- Applying the k - ω model to simulate turbulent steady flow in a channel
- Comparison of the numerical results with the theoretical study of internal flows
- Numerical solution of the unsteady turbulent Navier-Stokes equations and explanation of the phenomenon of intermittency through computational results

APPENDIX A

APPENDIX

A.1 URANS Discretization

The URANS equations are being discretized by the FVM as follows.

Continuity equation:

$$\begin{aligned} \iint_{CV} \frac{\partial u}{\partial x} dx dy &= \int_w^e \frac{\partial u}{\partial x} dx \int_s^n 1 dy = u|_w^e \Delta y = (u_e - u_w) \Delta y \\ &= \left(\frac{u_E + u_P}{2} - \frac{u_P + u_W}{2} \right) \Delta y = \frac{(u_E - u_W)}{2} \Delta y \end{aligned}$$

$$\begin{aligned} \iint_{CV} \frac{\partial v}{\partial y} dx dy &= \int_s^n \frac{\partial v}{\partial y} dy \int_w^e 1 dx = v|_s^n \Delta x = (v_n - v_s) \Delta x \\ &= \left(\frac{v_N + v_P}{2} - \frac{v_P + v_S}{2} \right) \Delta x = \frac{(v_N - v_S)}{2} \Delta x \end{aligned}$$

x-momentum For the **Pressure** term it holds that:

$$\iint_{CV} \frac{\partial P}{\partial x} dx dy = (P_E - P_P) \Delta y$$

Convective terms: To discretize the convective terms we have to transform them into their closed form as we are going to show for the $k-\omega$ equations.

$$u \frac{\partial u}{\partial x} + v \frac{\partial u}{\partial y} \quad (\text{closed-form}) \quad = \quad \frac{\partial u^2}{\partial x} + \frac{\partial (uv)}{\partial y}$$

$$\begin{aligned}\iint_{\text{CV}} \frac{\partial u^2}{\partial x} dx dy &= \int_w^e \frac{\partial u^2}{\partial x} dx \int_s^n 1 dy = u^2|_w^e \Delta y = (u_e^2 - u_w^2) \Delta y \\ &= \left(\frac{u_E^2 + u_P^2}{2} - \frac{u_P^2 + u_W^2}{2} \right) \Delta y = \frac{(u_E^2 - u_W^2)}{2} \Delta y\end{aligned}$$

$$\begin{aligned}\iint_{\text{CV}} \frac{\partial(uv)}{\partial y} dx dy &= \int_s^n \frac{\partial(uv)}{\partial y} dy \int_w^e 1 dx = uv|_s^n \Delta x \\ &= \left(\frac{u_P v_P + u_N v_N}{2} - \frac{u_P v_P + u_S v_S}{2} \right) \Delta x = \frac{(u_N v_N - u_S v_S)}{2} \Delta x\end{aligned}$$

Viscous terms:

$$\begin{aligned}\iint_{\text{CV}} \frac{\partial}{\partial y} \left[(\nu + \varepsilon_t) \frac{\partial u}{\partial y} \right] dy dx &= \int_s^n \frac{\partial}{\partial y} \left[(\nu + \varepsilon_t) \frac{\partial u}{\partial y} \right] dy \int_w^e 1 dx \\ &= \left(\left[(\nu + \varepsilon_t) \frac{\partial u}{\partial y} \right]_n - \left[(\nu + \varepsilon_t) \frac{\partial u}{\partial y} \right]_s \right) \Delta x \\ &= \left[(\nu + (\varepsilon_t)_n) \frac{u_N - u_P}{\Delta y} - (\nu + (\varepsilon_t)_s) \frac{u_P - u_S}{\Delta y} \right] \Delta x,\end{aligned}$$

$$\begin{aligned}\iint_{\text{CV}} \frac{\partial}{\partial x} \left[(\nu + \varepsilon_t) \frac{\partial u}{\partial x} \right] dx dy &= \int_w^e \frac{\partial}{\partial x} \left[(\nu + \varepsilon_t) \frac{\partial u}{\partial x} \right] dx \int_s^n 1 dy \\ &= \left(\left[(\nu + \varepsilon_t) \frac{\partial u}{\partial x} \right]_e - \left[(\nu + \varepsilon_t) \frac{\partial u}{\partial x} \right]_w \right) \Delta y \\ &= \left[(\nu + (\varepsilon_t)_e) \frac{u_E - u_P}{\Delta x} - (\nu + (\varepsilon_t)_w) \frac{u_P - u_W}{\Delta x} \right] \Delta y,\end{aligned}$$

For the **Time Dependent Term:**

$$\iint_{\text{CV}} \frac{\partial u}{\partial t} dx dy = \frac{u_{\text{p}^{new}} - u_{\text{p}^{old}}}{\Delta t} \Delta x \Delta y$$

y-momentum:

$$\iint_{\text{CV}} \frac{\partial P}{\partial y} dy dx = (P_N - P_p) \Delta y$$

Convective terms: To discretize the convective terms we have to transform them into their closed form as we are going to show for the k- ω equations.

$$u \frac{\partial v}{\partial x} + v \frac{\partial v}{\partial y} \quad (\text{closed-form}) \quad = \quad \frac{\partial v^2}{\partial y} + \frac{\partial(uv)}{\partial x}$$

$$\begin{aligned} \iint_{\text{CV}} \frac{\partial v^2}{\partial y} dx dy &= \int_s^n \frac{\partial v^2}{\partial y} dy \int_w^e 1 dx = v^2|_s^n \Delta x = (v_n^2 - v_s^2) \Delta x \\ &= \left(\frac{v_N^2 + v_P^2}{2} - \frac{v_P^2 + v_S^2}{2} \right) \Delta x = \frac{(u_N^2 - u_S^2)}{2} \Delta x \end{aligned}$$

$$\begin{aligned} \iint_{\text{CV}} \frac{\partial(uv)}{\partial x} dx dy &= \int_w^e \frac{\partial(uv)}{\partial x} dx \int_s^n 1 dy = uv|_w^e \Delta y \\ &= \left(\frac{u_P v_P + u_E v_E}{2} - \frac{u_P v_P + u_W v_W}{2} \right) \Delta y = \frac{(u_E v_E - u_W v_W)}{2} \Delta y \end{aligned}$$

Viscous terms:

$$\begin{aligned} \iint_{\text{CV}} \frac{\partial}{\partial y} \left[(\nu + \varepsilon_t) \frac{\partial v}{\partial y} \right] dy dx &= \int_s^n \frac{\partial}{\partial y} \left[(\nu + \varepsilon_t) \frac{\partial v}{\partial y} \right] dy \int_w^e 1 dx \\ &= \left(\left[(\nu + \varepsilon_t) \frac{\partial v}{\partial y} \right]_n - \left[(\nu + \varepsilon_t) \frac{\partial v}{\partial y} \right]_s \right) \Delta x \\ &= \left[(\nu + (\varepsilon_t)_n) \frac{v_N - v_P}{\Delta y} - (\nu + (\varepsilon_t)_s) \frac{v_P - v_S}{\Delta y} \right] \Delta x, \end{aligned}$$

$$\begin{aligned} \iint_{\text{CV}} \frac{\partial}{\partial x} \left[(\nu + \varepsilon_t) \frac{\partial v}{\partial x} \right] dx dy &= \int_w^e \frac{\partial}{\partial x} \left[(\nu + \varepsilon_t) \frac{\partial v}{\partial x} \right] dx \int_s^n 1 dy \\ &= \left(\left[(\nu + \varepsilon_t) \frac{\partial v}{\partial x} \right]_e - \left[(\nu + \varepsilon_t) \frac{\partial v}{\partial x} \right]_w \right) \Delta y \\ &= \left[(\nu + (\varepsilon_t)_e) \frac{v_E - v_P}{\Delta x} - (\nu + (\varepsilon_t)_w) \frac{v_P - v_W}{\Delta x} \right] \Delta y, \end{aligned}$$

For the **Time Dependent Term:**

$$\iint_{\text{CV}} \frac{\partial v}{\partial t} dx dy = \frac{v_{\text{p}^{new}} - v_{\text{p}^{old}}}{\Delta t} \Delta x \Delta y$$

A.2 k - ω Turbulence model Cartesian Form

The k - ω model that is studied is this of Wilcox (1988) as it is described in his work. To convert the k - ω equations into a closed Cartesian form, we must make two observations. First, we have to convert the inertia terms on the left hand-side of the equations into their closed Cartesian form. This process is made with the help of the continuity equation.

$$\frac{\partial(uk)}{\partial x} = u \frac{\partial k}{\partial x} + k \frac{\partial u}{\partial x} \Rightarrow u \frac{\partial k}{\partial x} = \frac{\partial(uk)}{\partial x} - k \frac{\partial u}{\partial x} \quad (\text{A.1})$$

$$\frac{\partial(vk)}{\partial y} = v \frac{\partial k}{\partial y} + k \frac{\partial v}{\partial y} \Rightarrow v \frac{\partial k}{\partial y} = \frac{\partial(vk)}{\partial y} - k \frac{\partial v}{\partial y} \quad (\text{A.2})$$

By adding:

$$(A.1) + (A.2) \Rightarrow u \frac{\partial k}{\partial x} + v \frac{\partial k}{\partial y} = \frac{\partial(uk)}{\partial x} + \frac{\partial(vk)}{\partial y} - k \left(\frac{\partial u}{\partial x} + \frac{\partial v}{\partial y} \right) \quad (\text{A.3})$$

The last term of equation A.3 vanishes due to the continuity equation for incompressible fluid. So, the convective terms can be replaced by the following relation:

$$u \frac{\partial k}{\partial x} + v \frac{\partial k}{\partial y} = \frac{\partial(uk)}{\partial x} + \frac{\partial(vk)}{\partial y} \quad (\text{A.4})$$

By the previous process it can be proven that:

$$u \frac{\partial \omega}{\partial x} + v \frac{\partial \omega}{\partial y} = \frac{\partial(u\omega)}{\partial x} + \frac{\partial(v\omega)}{\partial y} \quad (\text{A.5})$$

Another critical observation is to correctly define the **Production Term (P)**, which is calculated as follows [23]:

$$P = \tau_{ij} \frac{\partial u_i}{\partial x_j} = \rho \varepsilon_t S^2 = \frac{k}{\omega} \left(\frac{\partial u}{\partial y} + \frac{\partial v}{\partial x} \right)^2. \quad (\text{A.6})$$

The final k - ω equations in closed form are given by the following expressions:

- **Turbulence Kinetic Energy (TKE):**

$$\begin{aligned} \frac{\partial k}{\partial t} + \frac{\partial(uk)}{\partial x} + \frac{\partial(vk)}{\partial y} &= \frac{k}{\omega} \left(\frac{\partial u}{\partial y} + \frac{\partial v}{\partial x} \right)^2 - \beta^* k \omega \\ &+ \frac{\partial}{\partial x} \left[\left(\nu + \sigma^* \frac{k}{\omega} \right) \frac{\partial k}{\partial x} \right] + \frac{\partial}{\partial y} \left[\left(\nu + \sigma^* \frac{k}{\omega} \right) \frac{\partial k}{\partial y} \right] \end{aligned} \quad (\text{A.7}).$$

- **Specific Dissipation Rate:**

$$\begin{aligned} \frac{\partial \omega}{\partial t} + \frac{\partial(u\omega)}{\partial x} + \frac{\partial(v\omega)}{\partial y} &= \alpha \left(\frac{\partial u}{\partial y} + \frac{\partial v}{\partial x} \right)^2 - \beta \omega^2 \\ &+ \frac{\partial}{\partial x} \left[\left(\nu + \sigma \frac{k}{\omega} \right) \frac{\partial \omega}{\partial x} \right] + \frac{\partial}{\partial y} \left[\left(\nu + \sigma \frac{k}{\omega} \right) \frac{\partial \omega}{\partial y} \right] \end{aligned} \quad (\text{A.8}).$$

- **Closure Coefficients and Auxiliary Relations:**

$$\varepsilon_t = \frac{k}{\omega}, \quad \alpha = \frac{5}{9}, \quad \beta = \frac{3}{40}, \quad \beta^* = \frac{9}{100}, \quad \sigma = \sigma^* = \frac{1}{2}$$

A.3 Discretization of k - ω equations

A.3.1 Discretization of k equation

Convective terms

- $$\begin{aligned} \iint_{CV} \frac{\partial(vk)}{\partial y} dy dx &= \int_s^n \frac{\partial(vk)}{\partial y} dy \int_w^e 1 dx = [vk]_s^n \Delta x \\ &= \left(\frac{v_P k_P + v_N k_N}{2} - \frac{v_P k_P + v_S k_S}{2} \right) \Delta x = (v_N k_N - v_S k_S) \frac{\Delta x}{2} \end{aligned}$$
- $$\begin{aligned} \iint_{CV} \frac{\partial(uk)}{\partial x} dx dy &= \int_w^e \frac{\partial(uk)}{\partial x} dx \int_s^n 1 dy = [uk]_w^e \Delta y \\ &= \left(\frac{u_P k_P + u_E k_E}{2} - \frac{u_P k_P + u_W k_W}{2} \right) \Delta y = (u_E k_E - u_W k_W) \frac{\Delta y}{2} \end{aligned}$$

- $$\begin{aligned} \iint_{CV} \frac{\partial v}{\partial x} dx dy &= \int_w^e \frac{\partial v}{\partial x} dx \int_s^n 1 dy = v \Big|_w^e \Delta y = (v_e - v_w) \Delta y \\ &= \left(\frac{v_E + u_P}{2} - \frac{v_P + v_W}{2} \right) \Delta y = \frac{(v_E - v_W) \Delta y}{2} \end{aligned}$$
- $$\begin{aligned} \iint_{CV} \frac{\partial u}{\partial y} dx dy &= \int_s^n \frac{\partial u}{\partial y} dy \int_w^e 1 dx = u \Big|_s^n \Delta x = (u_n - u_s) \Delta x \\ &= \left(\frac{u_N + u_P}{2} - \frac{u_P + u_S}{2} \right) \Delta x = \frac{(u_N - u_S) \Delta x}{2} \end{aligned}$$

For the **Viscous Terms**:

•

$$\begin{aligned} \iint_{\text{CV}} \frac{\partial}{\partial y} \left[\left(\nu + \sigma^* \frac{k}{\omega} \right) \frac{\partial k}{\partial y} \right] dy dx &= \int_s^n \frac{\partial}{\partial y} \left[\left(\nu + \sigma^* \frac{k}{\omega} \right) \frac{\partial k}{\partial y} \right] dy \int_w^e 1 dx \\ &= \left[\left(\nu + \sigma^* \frac{k}{\omega} \right) \frac{\partial k}{\partial y} \right]_s^n \Delta x = \left(\left[\left(\nu + \sigma^* \frac{k}{\omega} \right) \frac{\partial k}{\partial y} \right]_n - \left[\left(\nu + \sigma^* \frac{k}{\omega} \right) \frac{\partial k}{\partial y} \right]_s \right) \Delta x \\ &= \left[\left(\nu + \left[\sigma^* \frac{k}{\omega} \right]_n \right) \frac{k_N - k_P}{\Delta y} - \left(\nu + \left[\sigma^* \frac{k}{\omega} \right]_s \right) \frac{k_P - k_S}{\Delta y} \right] \Delta x \end{aligned}$$

•

$$\begin{aligned} \iint_{\text{CV}} \frac{\partial}{\partial x} \left[\left(\nu + \sigma^* \frac{k}{\omega} \right) \frac{\partial k}{\partial x} \right] dx dy &= \int_w^e \frac{\partial}{\partial x} \left[\left(\nu + \sigma^* \frac{k}{\omega} \right) \frac{\partial k}{\partial x} \right] dx \int_s^n 1 dy \\ &= \left[\left(\nu + \sigma^* \frac{k}{\omega} \right) \frac{\partial k}{\partial x} \right]_w^e \Delta y = \left(\left[\left(\nu + \sigma^* \frac{k}{\omega} \right) \frac{\partial k}{\partial x} \right]_e - \left[\left(\nu + \sigma^* \frac{k}{\omega} \right) \frac{\partial k}{\partial x} \right]_w \right) \Delta y \\ &= \left[\left(\nu + \left[\sigma^* \frac{k}{\omega} \right]_e \right) \frac{k_E - k_P}{\Delta x} - \left(\nu + \left[\sigma^* \frac{k}{\omega} \right]_w \right) \frac{k_P - k_W}{\Delta x} \right] \Delta y \end{aligned}$$

For the **Time Dependent Term**:

$$\iint_{\text{CV}} \frac{\partial k}{\partial t} dx dy = \frac{k_{\text{p}^{new}} - k_{\text{p}^{old}}}{\Delta t} \Delta x \Delta y$$

The final discretized form of the k -equation is presented as follows:

$$\begin{aligned} &\frac{k_{\text{p}^{new}} - k_{\text{p}^{old}}}{\Delta t} \Delta x \Delta y + (u_E k_E - u_W k_W) \frac{\Delta y}{2} + (v_N k_N - v_S k_S) \frac{\Delta x}{2} \\ &- \Delta x \Delta y \frac{k_P}{\omega_P} \left(\frac{(v_E - v_W) \Delta y}{2} + \frac{(u_N - u_S) \Delta x}{2} \right)^2 + \beta^* k_P \omega_P \Delta x \Delta y \\ &- \left[\left(\nu + \sigma^* \frac{k_E + k_P}{\omega_E + \omega_P} \right) \frac{k_E - k_P}{\Delta x} - \left(\nu + \sigma^* \frac{k_P + k_W}{\omega_P + \omega_W} \right) \frac{k_P - k_W}{\Delta x} \right] \Delta y \\ &- \left[\left(\nu + \sigma^* \frac{k_N + k_P}{\omega_N + \omega_P} \right) \frac{k_N - k_P}{\Delta y} - \left(\nu + \sigma^* \frac{k_P + k_S}{\omega_P + \omega_S} \right) \frac{k_P - k_S}{\Delta y} \right] \Delta x = 0 \end{aligned}$$

A.4 Discretization of ω equation

Convective terms

- $$\begin{aligned} \iint_{\text{CV}} \frac{\partial(u\omega)}{\partial x} dx dy &= \int_w^e \frac{\partial(u\omega)}{\partial x} dx \int_s^n 1 dy = [u\omega]_w^e \Delta y \\ &= \left(\frac{u_E \omega_E + u_P \omega_P}{2} - \frac{u_P \omega_P + u_W \omega_W}{2} \right) \Delta y = \frac{(u_E \omega_E - u_W \omega_W)}{2} \Delta y \end{aligned}$$
- $$\begin{aligned} \iint_{\text{CV}} \frac{\partial(v\omega)}{\partial y} dy dx &= \int_s^n \frac{\partial(v\omega)}{\partial y} dy \int_w^e 1 dx = [v\omega]_s^n \Delta x \\ &= \left(\frac{v_N \omega_N + v_P \omega_P}{2} - \frac{v_P \omega_P + v_S \omega_S}{2} \right) \Delta x = \frac{(v_N \omega_N - v_S \omega_S)}{2} \Delta x \end{aligned}$$
- $$\begin{aligned} \iint_{\text{CV}} \frac{\partial v}{\partial x} dx dy &= \int_w^e \frac{\partial v}{\partial x} dx \int_s^n 1 dy = v|_w^e \Delta y = (v_e - v_w) \Delta y \\ &= \left(\frac{v_E + v_P}{2} - \frac{v_P + v_W}{2} \right) \Delta y = \frac{(v_E - v_W)}{2} \Delta y \end{aligned}$$
- $$\begin{aligned} \iint_{\text{CV}} \frac{\partial u}{\partial y} dx dy &= \int_s^n \frac{\partial u}{\partial y} dy \int_w^e 1 dx = u|_s^n \Delta x = (u_n - u_s) \Delta x \\ &= \left(\frac{u_N + u_P}{2} - \frac{u_P + u_S}{2} \right) \Delta x = \frac{(u_N - u_S)}{2} \Delta x \end{aligned}$$

For the **Viscous Terms**:

- $$\begin{aligned} \iint_{\text{CV}} \frac{\partial}{\partial y} \left[\left(\nu + \sigma^* \frac{k}{\omega} \right) \frac{\partial \omega}{\partial y} \right] dy dx &= \int_s^n \frac{\partial}{\partial y} \left[\left(\nu + \sigma^* \frac{k}{\omega} \right) \frac{\partial \omega}{\partial y} \right] dy \int_w^e 1 dx \\ &= \left[\left(\nu + \sigma^* \frac{k}{\omega} \right) \frac{\partial \omega}{\partial y} \right]_s^n \Delta x = \left(\left[\left(\nu + \sigma^* \frac{k}{\omega} \right) \frac{\partial \omega}{\partial y} \right]_n - \left[\left(\nu + \sigma^* \frac{k}{\omega} \right) \frac{\partial \omega}{\partial y} \right]_s \right) \Delta x \\ &= \left[\left(\nu + \left[\sigma^* \frac{k}{\omega} \right]_n \right) \frac{\omega_N - \omega_P}{\Delta y} - \left(\nu + \left[\sigma^* \frac{k}{\omega} \right]_s \right) \frac{\omega_P - \omega_S}{\Delta y} \right] \Delta x \end{aligned}$$

where the fractions are calculated by the following expressions:

$$\left(\frac{k}{\omega}\right)_n = \frac{k_N + k_P}{\omega_N + \omega_P}, \quad \left(\frac{k}{\omega}\right)_s = \frac{k_S + k_P}{\omega_S + \omega_P}$$

•

$$\begin{aligned} & \iint_{CV} \frac{\partial}{\partial x} \left[\left(\nu + \sigma^* \frac{k}{\omega} \right) \frac{\partial \omega}{\partial x} \right] dx dy = \int_w^e \frac{\partial}{\partial x} \left[\left(\nu + \sigma^* \frac{k}{\omega} \right) \frac{\partial \omega}{\partial x} \right] dx \int_s^n 1 dy \\ & = \left[\left(\nu + \sigma^* \frac{k}{\omega} \right) \frac{\partial \omega}{\partial x} \right]_w^e \Delta y = \left(\left[\left(\nu + \sigma^* \frac{k}{\omega} \right) \frac{\partial \omega}{\partial x} \right]_e - \left[\left(\nu + \sigma^* \frac{k}{\omega} \right) \frac{\partial \omega}{\partial x} \right]_w \right) \Delta y \\ & = \left[\left(\nu + \left[\sigma^* \frac{k}{\omega} \right]_e \right) \frac{\omega_E - \omega_P}{\Delta x} - \left(\nu + \left[\sigma^* \frac{k}{\omega} \right]_w \right) \frac{\omega_P - \omega_W}{\Delta x} \right] \Delta y \end{aligned}$$

where the fractions are calculated by the following expressions:

$$\left(\frac{k}{\omega}\right)_e = \frac{k_E + k_P}{\omega_E + \omega_P}, \quad \left(\frac{k}{\omega}\right)_w = \frac{k_W + k_P}{\omega_W + \omega_P}$$

For the **Time Dependent Term**:

$$\iint_{CV} \frac{\partial \omega}{\partial t} dx dy = \frac{\omega_{p^{new}} - \omega_{p^{old}}}{\Delta t} \Delta x \Delta y$$

The final discretized form of the ω -equation is presented as follows:

$$\begin{aligned} & \frac{\omega_{p^{new}} - \omega_{p^{old}}}{\Delta t} \Delta x \Delta y + (u_E k \omega_E - u_W \omega_W) \frac{\Delta y}{2} + (v_N \omega_N - v_S \omega_S) \frac{\Delta x}{2} \\ & - \alpha \Delta x \Delta y \left(\frac{(v_E - v_W) \Delta y}{2} + \frac{(u_N - u_S) \Delta x}{2} \right)^2 + \beta \omega_P^2 \Delta x \Delta y \\ & - \left[\left(\nu + \sigma^* \frac{k_E + k_P}{\omega_E + \omega_P} \right) \frac{\omega_E - \omega_P}{\Delta x} - \left(\nu + \sigma^* \frac{k_P + k_W}{\omega_P + \omega_W} \right) \frac{\omega_P - \omega_W}{\Delta x} \right] \Delta y \\ & - \left[\left(\nu + \sigma^* \frac{k_N + k_P}{\omega_N + \omega_P} \right) \frac{\omega_N - \omega_P}{\Delta y} - \left(\nu + \sigma^* \frac{k_P + k_S}{\omega_P + \omega_S} \right) \frac{\omega_P - \omega_S}{\Delta y} \right] \Delta x = 0 \end{aligned}$$

BIBLIOGRAPHY

- [1] ABDOU, M. A. M. The reynolds number: A journey from its origin to modern applications. *Fluids* 7, 6 (2022), 181.
- [2] BISTAFA, S. R. On the development of the Navier-Stokes equations. *Revista Brasileira de Ensino de Física* (2018).
- [3] BONKILE, M. P., AWASTHI, A., LAKSHMI, C., MUKUNDAN, V., AND ASWIN, V. S. A systematic literature review of burgers' equation with recent advances. *Pramana – Journal of Physics* 91, 2 (2018), 25.
- [4] BORITCHEV, A. Decaying turbulence in the generalised burgers equation. *Archive for Rational Mechanics and Analysis* 214 (2014), 331–357.
- [5] CHEN, S., FENG, S., FU, W., AND ZHANG, Y. Logistic map: Stability and entrance to chaos. *Journal of Physics: Conference Series*.
- [6] DAVIDSON, P. A. *Turbulence: An Introduction for Scientists and Engineers*, 2nd ed. Oxford University Press, Oxford, United Kingdom, 2015. Introduction to concepts in turbulence and Navier-Stokes equations.
- [7] DE, S., MITRA, D., AND PANDIT, R. Dynamic multiscaling in stochastically forced burgers turbulence. *Scientific Reports* 13 (2023), 7151.
- [8] FELIAS, A. C., KYRIAKOUDI, K. C., MPIRAKI, K. N., AND XENOS, M. A. Analytic and numerical solutions to nonlinear partial differential equations in biomechanics. In *Analysis, Geometry, Nonlinear Optimization and Applications*. World Scientific, 2023, pp. 331–403.

- [9] FERZIGER, J. H., AND PERIĆ, M. *Computational Methods for Fluid Dynamics*, 3rd ed. Springer, 2002.
- [10] HIRSCH, M. W., SMALE, S., AND DEVANEY, R. L. *Differential Equations, Dynamical Systems, and an Introduction to Chaos*, 3rd ed. Academic Press, Waltham, MA, USA, 2013.
- [11] KOUTSOYIANNIS, D. A power-law approximation of the turbulent flow friction factor useful for the design and simulation of urban water networks. *Urban Water Journal* 4, 4 (2007), 291–301.
- [12] KOWALCZUK, Z., AND TATARA, M. S. Analytical ‘steady-state’-based derivation and clarification of the courant–friedrichs–lewy condition for pipe flow. *Journal of Natural Gas Science and Engineering* 96 (2021), 104241.
- [13] KUMAR, N. K. A review on burgers’ equations and its applications. *Journal of Institute of Science and Technology* 28, 2 (2023), 123–133.
- [14] MENTER, F. R. Two-equation eddy-viscosity turbulence models for engineering applications. *AIAA Journal* 32, 8 (1994), 1598–1605.
- [15] MORKOVIN, M. V. Bypass transition to turbulence and research desiderata. Tech. rep., Illinois Institute of Technology, 1985. NASA Technical Report.
- [16] MOUKALLED, F., MANGANI, L., AND DARWISH, M. *The Finite Volume Method in Computational Fluid Dynamics*, vol. 113 of *Fluid Mechanics and Its Applications*. Springer International Publishing, Switzerland, 2016.
- [17] MUNSON, B. R., OKIISHI, T. H., HUEBSCH, W. W., AND ROTHMAYER, A. P. *Fundamentals of Fluid Mechanics*, 7th ed. John Wiley & Sons, Inc., 2013.
- [18] POPE, S. B. *Turbulent Flows*. Cambridge University Press, Cambridge, UK, 2000.
- [19] SCHLICHTING, H., AND GERSTEN, K. *Boundary-Layer Theory*. Springer Berlin Heidelberg, 2017.
- [20] SIMFLOW. Courant number in cfd. *SimFlow* (2023).

- [21] THOMPSON, J. F., WARSI, Z. U. A., AND MASTIN, C. W. *Numerical Grid Generation: Foundations and Applications*. Elsevier North-Holland, Inc., USA, 1985.
- [22] VERSTEEG, H., AND MALALASEKERA, W. *An Introduction to Computational Fluid Dynamics: The Finite Volume Method*, 2nd ed. Pearson Education Limited, Harlow, Essex, England, 2007.
- [23] WILCOX, D. C. *Turbulence Modeling for CFD*, 3rd ed. DCW Industries, Incorporated, 2006.
- [24] XENOS, M., AND TZIRTZILAKIS, E. *Fluid mechanics with applications*. Gotsis, 2018.
- [25] ΒΟΥΓΙΑΤΖΗΣ, , AND ΜΕΛΕΤΑΙΔΟΥ, *Εισαγωγή στα Μη Γραμμικά Δυναμικά Συστήματα*. Σύνδεσμος Ελληνικών Ακαδημαϊκών Βιβλιοθηκών - Κάλλιπος, Εθνικό Μετσόβιο Πολυτεχνείο, Ζωγράφου, 2015.
- [26] ΚΑΤΣΟΥΔΑΣ, Αριθμητικές λύσεις της τυρβώδους ροής σε εσωτερικές και εξωτερικές ροές. Master's thesis, Πανεπιστήμιο Ιωαννίνων, Τμήμα Μαθηματικών, 2024.
- [27] ΠΡΙΝΟΣ, *Υδραυλική Κλειστών & Ανοικτών Αγωγών*. Εκδόσεις Ζήτη, 2013.
- [28] ΣΚΟΥΤΑΡΗΣ, *Μερικές Διαφορικές Εξισώσεις*. Εκδόσεις Κορφιάτης, 2020.
- [29] ΣΟΥΡΛΑΣ, *Δυναμικά Συστήματα και Εφαρμογές με τη χρήση του Maple*. Πανεπιστήμιο Πατρών, 2010.